Pontifícia Universidade Católica do Rio Grande do Sul
Faculdade de Biociências
Programa de Pós-Graduação em Biologia Celular e Molecular

CAROLINE BRANCHER BORGES

Fosforribosilpirofosfato sintase de *Mycobacterium tuberculosis* tipo selvagem: uma PRS classe II bacteriana?

Porto Alegre
Setembro, 2011

Pontifícia Universidade Católica do Rio Grande do Sul
Faculdade de Biociências
Programa de Pós-Graduação em Biologia Celular e Molecular

Fosforribosilpirofosfato sintase de *Mycobacterium tuberculosis* tipo selvagem: uma PRS classe II bacteriana?

Dissertação apresentada ao Programa de Pós-Graduação em Biologia Celular e Molecular como requisito para a obtenção do grau de Mestre.

CAROLINE BRANCHER BORGES

Orientador:
Prof. Dr. Luiz Augusto Basso
Co-orientador:
Prof. Dr. Diógenes Santiago Santos

Porto Alegre
Setembro, 2011

CAROLINE BRANCHER BORGES

Fosforribosilpirofosfato sintase de *Mycobacterium tuberculosis* tipo selvagem: uma PRS classe II bacteriana?

Dissertação apresentada ao Programa de Pós-Graduação em Biologia Celular e Molecular como requisito para a obtenção do grau de Mestre.

Aprovada em ____de_____de_____.

BANCA EXAMINADORA:

Dr. Jeverson Frazzon – UFRGS

_____

Dr. Walter Filguera de Azevedo Jr – PUCRS

_____

Dr. André Arigony Souto Jr – PUCRS (relator)

_____

Agradecimentos

Agradeço aos meus orientadores Prof. Diógenes Santiago Santos e Prof. Luiz Augusto Basso pela oportunidade, ensinamentos e apoio dispensado na realização deste trabalho.

Ao Programa de Pós-Graduação em Biologia Celular e Molecular da PUCRS.

Aos colegas do CPBMF pelo carinho, amizade, apoio e força nos momentos mais difíceis, e que foram fundamentais para a realização deste trabalho.

Aos meus pais, Ladir e Ademir Brancher, que mesmo longe sempre me apoiaram. Agradeço pelos constantes ensinamentos, pelo estímulo e valores que serão para sempre importantes na minha vida.

Aos meus irmãos e toda a família pelo amor, carinho, compreensão, paciência e pela força para seguir em frente nos momentos difíceis.

Agradeço em especial ao meu marido André Vieira Borges, que sempre esteve ao meu lado, ajudando, incentivando, com carinho e dedicação, e mesmo nos momentos mais complicados me ajudou a encontrar uma resposta para as minhas dúvidas.

Agradeço, enfim, a todos que de alguma forma, contribuíram não só para a realização deste trabalho, como também para a minha formação pessoal e profissional.

Muito obrigada a todos.

Resumo

A tuberculose humana (TB), causada principalmente pelo *Mycobacterium tuberculosis*, representa uma ameaça global liderando a causa de morte em adultos em decorrência de um único agente infeccioso; sendo responsável por cerca de dois milhões de óbitos por ano no mundo. Estima-se que aproximadamente um terço da população está infectada com o bacilo na sua forma latente. Agentes quimioterápicos mais eficazes e menos tóxicos são necessários para reduzir a duração do tratamento atual, assim como melhorar as possibilidades de tratamento para as cepas MDR-TB, XDR-TB e TDR-TB. Além disso, há necessidade de um tratamento eficaz para a TB latente, impedindo ainda que a doença se desenvolva para a forma ativa. Em 1998 com o sequenciamento completo do genoma da cepa de *M. tuberculosis* H37Rv houve a possibilidade do estudo e validação de alvos moleculares para o desenho racional de drogas anti-TB. As enzimas que participam de vias metabólicas essenciais são alvos promissores para o desenvolvimento de novos quimioterápicos para o tratamento da TB. A proteína fosforribosilpirofosfato sintase de *M. tuberculosis* (PRS, EC 2.7.6.1) é uma enzima de central importância em muitas vias metabólicas em todas as células. A PRS catalisa a formação do PRPP e AMP a partir da R5P e ATP, onde o ATP irá doar um grupamento difosforil para a R5P. A amplificação, clonagem, expressão e purificação de *Mt*PRS permitiu a identificação de seu substrato doador difosforil GTP, CTP e UTP, além de ATP já descrito anteriormente, além da ausência da dependência de fosfato inorgânico (P_i) para a atividade enzimática. Ambas características nos indicam que *Mt*PRS pode ser classificada como uma PRS classe II, até agora somente identificada em plantas. Através do ensaio de ligação através de espectrometria de fluorescência, vimos que os substratos R5P, ATP e GTP e o produto AMP são capazes de se ligarem à enzima na sua forma livre, indicando um provável mecanismo sequencial aleatório para nucleotídeos de purina, com liberação sequencial ordenada dos produtos; e mecanismo sequencial ordenado para a ligação dos substratos e liberação dos produtos para nucleotídeos de pirimidina. As características que distinguem as enzimas PRS Classe II da Classe I, sendo que a classe I inclui todas as três isoformas *H. sapiens*, podem ser exploradas para desenvolver inibidores específicos para *Mt*PRS, tanto para a tuberculose ativa quanto para a latente.

Palavras-chave: Tuberculose, *Mt*PRS, PRS Classe II, fosforribosilpirofosfato sintase, 5-fosfo- α -D-ribose-1-difosfato.

Abstract

The human tuberculosis (TB), caused mainly by the *Mycobacterium tuberculosis* represents a global threat leading to death in adults caused by a single infectious agent, accounting for about two million deaths per year worldwide. It is estimated that approximately one third of the word population is latently infected with the bacillus. Chemotherapeutic agents that are more effective and less toxic are required to reduce the duration of current treatment, as well as to improve the cure rates for MDR-TB strains, TDR-TB and XDR-TB. In addition, there is a need for effective treatment for latent TB, preventing the disease to develop into the active form. In 1998 with the complete genome sequencing of the strain of *M. tuberculosis* H37Rv there was the possibility of the study and validation of specific molecular targets for the rational design of anti-TB drugs. The enzymes that participate in essential metabolic pathways are promising targets for the development of new chemotherapeutic agents for the treatment of TB. The protein phosphoribosylpyrophosphate synthase from *M. tuberculosis* (PRS, EC 2.7.6.1) is an enzyme of central importance in several metabolic pathways in all cells. PRS catalyzes the formation of AMP and PRPP from R5P and ATP, where ATP donates its diphosphoril group to R5P. The amplification, cloning, expression and purification *Mt*PRS allowed the identification of its substrates diphosphoril donors GTP, CTP and UTP, in addition to previously described ATP and the absence inorganic phosphate (P_i) requirement for enzyme's activity. Both these features indicate that *Mt*PRS can be classified as a Class II PRS, so far only identified in plants. Fluorescence spectrophotometer binding assays indicate that the R5P, ATP and GTP (substrates) and AMP (product) are able to bind to the enzyme in its free form, indicating a possible sequential random mechanism for purine nucleotides, with sequential ordered release of products, and sequential ordered mechanism for binding of substrates and release of products for pyrimidine nucleotides. Features that distinguish the enzymes PRS Class II Class I, keeping in mind that the Class I includes all three *H. sapiens* PRS isoforms, can be exploited to develop specific inhibitors for *Mt*PRS for both active and latent TB.

Keywords: Tuberculosis, *Mt*PRS, Class II PRS, phosphoribosylpyrophosphate synthase, 5-phospho- α-D-ribose -1- diphosphate

Lista de Abreviaturas e Siglas

ADP: difosfato de adenosina

AMP: monofosfato de adenosina ou ácido adenílico

APRT: adenina fosforribosiltransferase

ATP: trifosfato de adenosina

BCG: bacilo Calmette-Guérin

CTP: trifosfato de citidina

DNA: ácido desoxirribonucléico

DOTS: do inglês *Directly Observed Treatment Short Course*

EMB: etambutol

FAD: dinucleotídeo flavina-adenina

FPLC: do inglês *Fast Protein Liquid Cromatography*

GMP: monofosfato de guanosina ou ácido guanosílico

GTP: trifosfato de guanosina

GDP: difosfato de guanosina

HGPRT: hipoxantina-guanina fosforribosiltransferase

HIV: vírus da imunodeficiência humana

IMP: inosina monofosfato

INH: isoniazida

IPTG: isopropil β-D-tiogalactopiranosideo

MDR: multi-resistente a drogas

Mtb: *Mycobacterium tuberculosis*

*Mt*OPRT: orotato fosforribosil transferase de *Mycobacterium tuberculosis*

NAD: nicotinamida adenina dinucleotídeo

$NADP^+$: nicotinamida adenina dinucleotídeo fosfato

NADPH: nicotinamida adenina dinucleotídeo fosfato (forma reduzida)

OMS: Organização Mundial da Saúde

PCR: reação em cadeia da polimerase

P_i: pirofosfato

PyNP: pirimidina nucleosídeo fosforilase

PRPP: 5-fosfo- α -D-ribose-1-difosfato.

PRS: fosforribosilpirofosfato sintase

PZA: pirazinamida

RIF: rifampicina

RNA: ácido ribonucléico

SIDA: síndrome da imunodeficiência adquirida

TB: tuberculose

UMP: uridina monofosfato

UP: uridina fosforilase

UTP: trifosfato de uridina

XDR: extensivamente resistente a drogas

TDR: totalmente resistente a drogas

TP: timidina fosforilase

Lista de ilustrações

Sumário

1. Introdução

1.1 Tuberculose

A tuberculose (TB) é uma doença infecto-contagiosa causada principalmente pelo *Mycobacterium tuberculosis*, uma das espécies patogênicas do gênero *Mycobacterium*. Atualmente, este gênero possui cerca de 70 espécies conhecidas, sendo que poucas causam doenças no ser humano. Entre as espécies patogênicas estão *Mycobacterium tuberculosis*, *Mycobacterium bovis, Mycobacterium africanum e Mycobacterium leprae* [1].

TB é um problema antigo para civilização humana. Presume-se que o gênero *Mycobacterium* originou-se há mais de 150 milhões de anos e que o progenitor de *Mycobacterium tuberculosis* tenha sido contemporâneo e co-evoluído com os primeiros hominídeos do leste da África há 3 milhões de anos atrás. Já os representantes modernos de *M. tuberculosis* parecem ter se originado de um progenitor comum entre 15.000 a 30.000 anos atrás. Historiadores estabeleceram a existência da TB endêmica no Egito, na Índia e na China a partir de múmias datando de 5.000, 3.300 e 2.300 anos A.C. respectivamente [2].

A epidemia de TB na Europa teve seu início por volta do século 17, devido à alta densidade populacional e às baixas condições sanitárias. Estima-se que em 1650, 20% da população tenham morrido por causa da doença. Já no século 19, o *M. tuberculosis* parece ter sido responsável pela morte de 1/3 da população em Paris. Com o início das grandes navegações e com a colonização das Américas e da África sub-Saariana pelos europeus, a doença foi transmitida a populações africanas espalhando-se mundialmente [2, 3].

Em 1854, após escrever sua dissertação médica sobre TB, Hermann Brehmer, resolveu então criar o primeiro sanatório, com a crença de que uma alimentação saudável, exercícios e a altitude poderiam curar os pacientes internados que sofriam de TB. Esse modelo foi utilizado para a criação dos subsequentes sanatórios, principalmente na Europa e Estados Unidos [2, 4].

Apesar dos esforços de muitos estudiosos na definição dos sintomas, características, possíveis causas e forma de contágio da doença; apenas em 1882 o alemão Robert Koch (1843-1910) identificou o *M. tuberculosis* como o agente etiológico da TB. Trinta e nove anos depois, a vacina BCG (bacilo Calmette-Guérin) foi introduzida para uso em humanos, e tornou-se a principal estratégia profilática contra a TB [2, 4].

Com o surgimento dos antibióticos estreptomicina (década de 1940), isoniazida (década de 1950), etambutol (década de 1960), e rifampicina (década de 1960), a batalha contra a TB parecia ter sido finalmente ganha. Entretanto, nos meados da década de 1980, o número de casos nos Estados Unidos começou a aumentar novamente. O advento da SIDA (Síndrome da Imudeficiência Adquirida), combinada com a superpopulação e com as más condições de saneamento em muitas áreas urbanas, fez com que a TB voltasse a ser um grave problema de saúde pública. Assim, em 1993, a Organização Mundial da Saúde (OMS) declarou a TB em estado de emergência no mundo, sendo ainda hoje a maior causa de morte por doença infecciosa em adultos [5].

Segundo estimativas da OMS, dois bilhões de pessoas, correspondendo a um terço da população mundial, estão infectados com o *M. tuberculosis.* Destes, 8 milhões desenvolverão a doença e 2 milhões morrerão a cada ano

[5]. O Brasil encontra-se na lista dos 22 países responsáveis por 80% do total de casos de TB no mundo (**Figura 1**). Dados epidemiológicos indicam uma incidência global da TB em 137 por 100.000 habitantes em 2009, ou seja, 9,4 milhões de casos. Destes 9,4 milhões de casos de TB, estima-se que 1,1 milhões são pacientes HIV – positivos [6]. Segundo o Portal da Saúde do Ministério da Saúde, no Brasil há cerca de 57 milhões de pessoas infectadas e, em 2010, foram registrados 72 mil novos casos, com uma incidência de 37,8 por 100.000 habitantes e 4,7 mil óbitos [7].

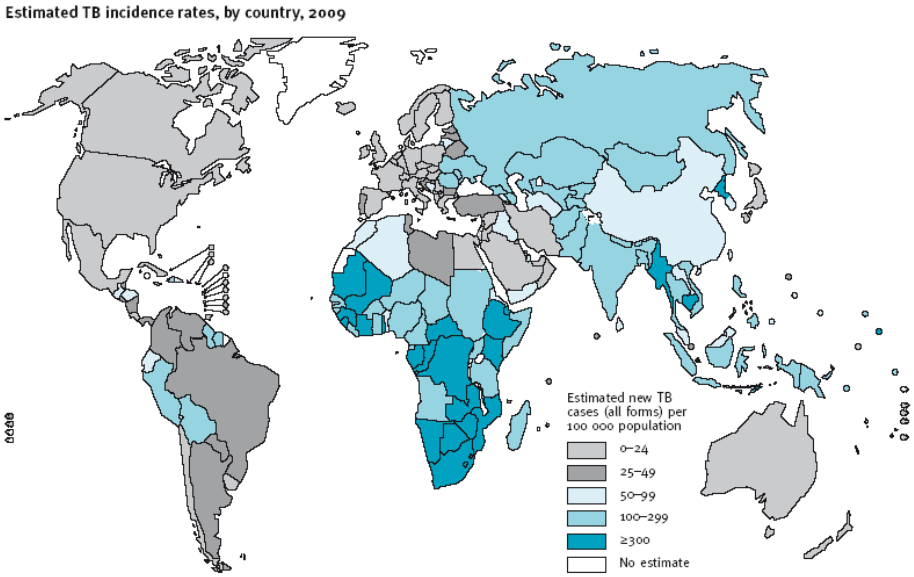

Figura 1: Estimativa das taxas de incidência de TB no mundo em 2009 de acordo com a Organização Mundial da Saúde (OMS) [6].

1.1.1 Patogenia

A forma mais comum de TB ataca os pulmões, mas também pode afetar a pleura, o sistema nervoso central, o sistema linfático, o sistema circulatório, o sistema urogenital, ossos, articulações e até mesmo a pele [8].

A principal forma de infecção da TB se dá através da tosse do paciente infectado (infecção ativa), em decorrência da inflamação pulmonar crônica, espirros e até mesmo através da fala, sendo expelidos aerossóis contendo o bacilo [9]. Um simples espirro pode expelir cerca de 40.000 gotículas [10].

A transmissão ocorre somente através de pessoas que possuem a forma ativa, não latente, de TB. A probabilidade da transmissão de uma pessoa para outra depende do número de partículas infecciosas expelidas pelo portador, a duração da exposição e a virulência da cepa de *M. tuberculosis* [11].

A TB também pode ser transmitida da mãe para o feto, antes ou durante o nascimento, ao respirar ou engolir o líquido amniótico infectado. Nos países em desenvolvimento, as crianças podem ser infectadas também por *M. bovis*, que pode estar presente no leite não pasteurizado. A cadeia de transmissão pode, todavia, ser quebrada, isolando pacientes com a doença ativa e iniciando uma terapia efetiva contra a TB [5].

1.1.2 Tratamento e resistência aos fármacos

A quimioterapia efetiva da TB deve incluir ação bactericida contra o crescimento rápido do organismo e subsequente esterilização dos bacilos dormentes. Entre os métodos de controle disponíveis para *M. tuberculosis* estão tratamento e diagnóstico precoces, tratamento da latência e a vacinação por BCG [12].

A OMS recomenda como tratamento o DOTS (do inglês *Directly Observed Treatment Short Course*) [6]. A quimioterapia consiste em uma associação de fármacos de primeira linha, isoniazida (INH), rifampicina (RIF), pirazinamida (PZA) e etambutol (EMB) durante dois meses, seguida por quatro

meses com INH e RIF [4, 13,14], podendo curar a maioria dos casos [4]. Além disso, a estratégia do DOTS inclui outros 5 componentes: i) estabelecer uma rede de indivíduos treinados a administrar e supervisionar o DOTS; ii) criar laboratórios e profissionais habilitados para o diagnóstico da TB; iii) implementar um sistema de fornecimento confiável de medicamentos de alta qualidade (preferencialmente, sem custo aos pacientes); iv) compromisso governamental e v) sistema de monitoramento dos casos, tratamento e resultados [2,13,15]. Essas estratégias previnem a ocorrência de novas infecções e, mais importante, dificultam o surgimento de casos MDR-TB (tuberculose multirresistente a drogas) [16].

A TB resistente a drogas normalmente surge através da seleção de cepas mutantes, decorrentes da quimioterapia inadequada, tendo uma relação direta com a disponibilidade de drogas e uma relação inversa com a eficácia do tratamento [17]. Os fatores mais importantes na emergência de resistência bacteriana a drogas incluem regime de tratamento não apropriado e não adesão à terapia prescrita [18].

Uma forma perigosa de TB é a MDR-TB, que é definida como resistência a no mínimo duas principais drogas anti-TB, INH e RIF. Em 2006, estimou-se 500 mil de casos por MDR-TB [17]. Enquanto a MDR-TB é geralmente tratável, requerendo uma quimioterapia prolongada e mais cara, usando drogas de segunda linha que provocam efeitos colaterais mais severos; as cepas denominadas de XDR-TB (tuberculose extensivamente resistente a drogas), definidas como resistentes a no mínimo RIF, INH, uma droga injetável de segunda linha (capreomicina, canamicina ou amicacina) e uma fluoroquinolona, são cepas virtualmente intratáveis [17]. Novos dados de XDR-TB confirmam

que essa forma de TB foi detectada em 45 países até o momento [19]. Recentemente, Velayati e colaboradores [20] documentaram o surgimento de novas formas de bacilos encontrados em pacientes diagnosticados com TB-MDR. Esses isolados foram classificados como linhagens totalmente resistentes às drogas (TDR), uma vez que apresentaram resistência *in vitro* a todas as drogas de primeira e segunda linha testadas. Durante o estudo, os pacientes infectados não responderam a nenhuma terapia padrão e permaneceram com culturas positivas após 18 meses de tratamento com drogas de segunda linha [20].

O aparecimento das cepas resistentes MDR-TB, XDR-TB e TDR-TB, especialmente em áreas onde pacientes estão infectados com o HIV, confirmam a necessidade de fortalecer a terapia básica antituberculose (anti-TB) [21].

Diante de tal cenário, há uma urgente necessidade de desenvolvimento de novas drogas anti-TB, além da aprovação e uso das que já estão em desenvolvimento [15].

1.1.3 Desenvolvimento de novas drogas anti-TB

Agentes quimioterápicos mais eficazes e menos tóxicos são necessários para reduzir o tempo do tratamento atual, possibilitando melhores tratamentos para a MDR-TB e XDR-TB. Além disso, há a necessidade de um tratamento eficaz para a TB latente, impedindo que a doença se desenvolva para a forma ativa, e também drogas que não interfiram com os anti-retrovirais, para que possam ser utilizados em pacientes co-infectados com HIV. A urgência no desenvolvimento de um tratamento mais eficaz para a TB se deve

principalmente ao fato de o tratamento atualmente recomendado pela OMS ter sido incapaz de controlar a TB no mundo [22].

Em 1998 com o sequenciamento completo do genoma da cepa de *M. tuberculosis* H37Rv [23] houve a possibilidade do estudo e validação de alvos moleculares para o desenho racional de drogas anti-TB. As enzimas que participam de vias metabólicas essenciais são alvos promissores para o desenvolvimento de novos quimioterápicos para o tratamento da TB.

1.2 Via da pentose-fosfato

A via da pentose-fosfato é uma via alternativa de oxidação das hexoses, independentemente da glicólise, está presente em muitos organismos e, em mamíferos, especialmente no fígado. No músculo, onde os carboidratos são utilizados quase que exclusivamente na geração de energia, as enzimas desta via não são encontradas. As principais funções dessa via são: a produção de NADPH e ribose-5-fosfato. A via permite a transformação da glicose em pentoses, através da síntese de ribose-5-fosfato, para a produção de nucleotídeos [24].

Contrariamente ao processo de glicólise, a oxidação neste processo não necessita de ATP e só se realiza em condições aeróbicas, uma vez que a reoxidação das coenzimas só é possível através do sistema transportador de elétrons ou de reações de biossíntese que usem o NADPH [24]. Esta via consiste nos componentes oxidativos e não oxidativos [25], conforme mostra a **Figura 2**.

1.2.1 Fase não oxidativa

Nesta ocorrem transferências de grupos com três átomos de carbono (transaldolisação) e com dois átomos de carbono (transcetolização) [27].

A transaldolase é uma enzima que, a semelhança da aldolase na glicólise, intervém em uma reação em que o grupo da enzima se liga ao substrato, o que permite, posteriormente, uma ruptura de ligações seguida de uma condensação (na glicólise havia apenas a ruptura da ligação) [24].

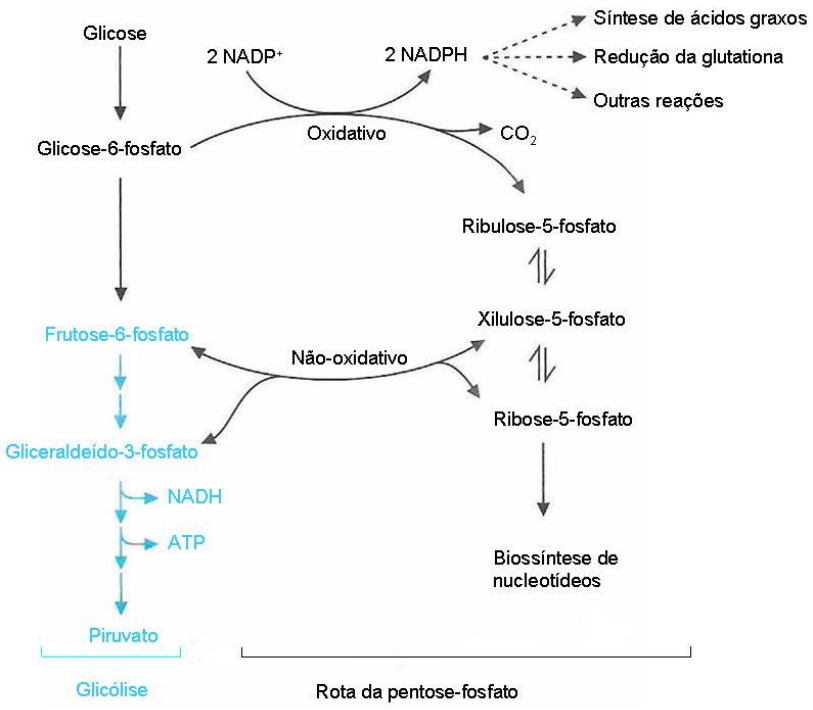

Figura 2: Visão geral da via de pentose-fosfato. A rota da pentose-fosfato produz NADPH para reações que necessitam de equivalentes de redução (elétrons) ou ribose-5-fosfato para a biossíntese de nucleotídeos. A porção da glicólise que não é parte da rota da pentose-fosfato é mostrada em azul. Adaptado de Smith *et al.* (2007) [26].

1.2.2 Fase oxidativa

A glicose-6-fosfato é oxidada a ribulose-5-fosfato com formação de NADPH. Na primeira reação, a glicose-6-fosfato sofre a ação da enzima glicose-6 fosfato-desidrogenase formando-se ácido-6-fosfoglucônico, que sofre uma descarboxilação oxidante originando ribulose-5-fosfato, catalisada pela 6-fosfogluconato-desidrogenase.

Nesta fase ocorrem duas oxidações com formação de NADPH, em que os elétrons serão transferidos para o sistema de transporte de elétrons com produção de 3 a 5 ATP, apesar do objetivo principal desta via não ser a produção de ATP. Em seguida, ocorre a isomerização em ribose-5-fosfato, por

intervenção da fosfopentose-epimerase [24]. Com isso ocorre a formação do PRPP a partir de ribose-5-fosfato e ATP, através da reação catalisada pela enzima fosforribosilpirofosfato sintase.

1.3 A enzima Fosforribosilpirofosfato sintase de *Mycobacterium tuberculosis*

A proteína fosforribosilpirofosfato sintase de *M. tuberculosis* (PRS, EC 2.7.6.1) é uma enzima de central importância em muitas vias metabólicas em todas as células, e as evidências acumuladas indicam que as enzimas PRS formam uma família complexa de isoenzimas com localização intracelular (citoplasma e núcleo), e diferentes características de dependência de fosfato [28, 29].

Na primeira etapa da biossíntese *de novo* de purina, a PRS ativa ribose-5-fosfato, combinando-a com ATP para formar 5-fosfo-α-D-ribose-1-difosfato (PRPP; **Figura 3**). Essa reação, que ocorre por um ataque nucleofílico do grupo C1-OH da ribose-5-fosfato no P_{β} do ATP é incomum já que um grupo pirofosforribosil é diretamente transferido do ATP para o C1 da ribose-5-fosfato e que o produto possui a configuração α anomérica. Como é esperado de uma enzima em tão importante etapa biossintética, a atividade da PRS varia com as concentrações de vários metabólitos, incluindo fosfato inorgânico e 2,3-difosfoglicerato, os quais são ativadores, e ADP e GDP, os quais são inibidores mistos [27].

A atividade da PRS irá depender da concentração intracelular dos produtos finais de diversas vias em que o PRPP é substrato. O aumento nos níveis de PRPP intracelular irá aumentar a síntese *de novo* de purinas. Por exemplo, em pacientes com deficiência de HGPRT (do inglês *hypoxanthine-guanine phosphoribosyl transferase*), os fibroblastos mostrarão uma aceleração nas taxas de formação de purina. O paciente com gota irá apresentar um aumento na atividade catalítica com aumento da produção de PRPP [30].

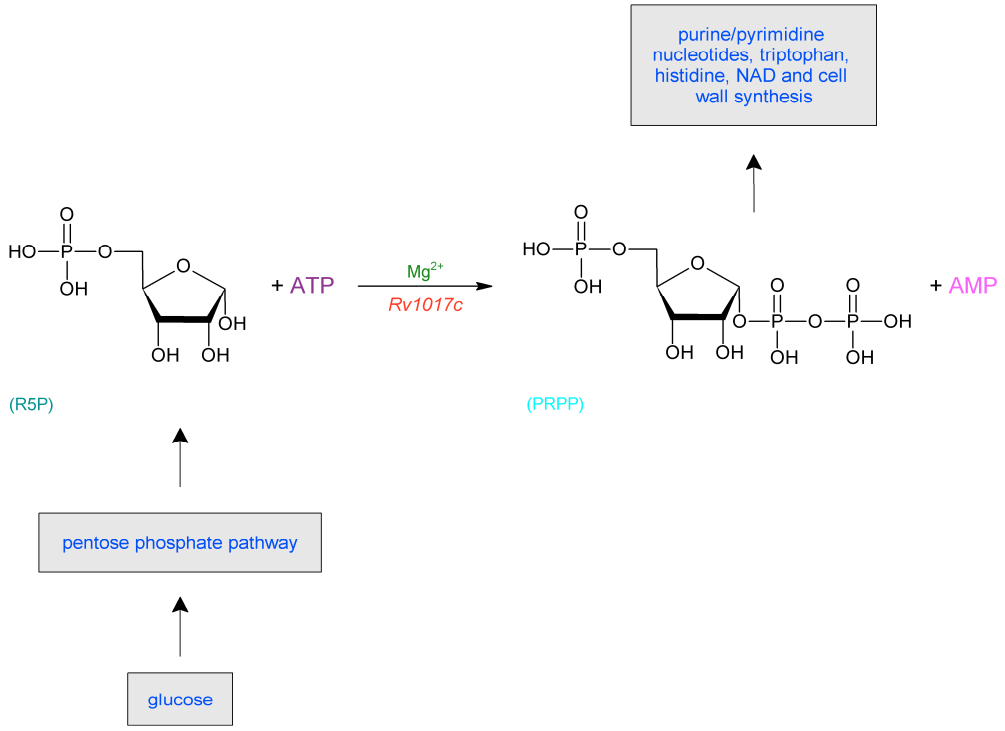

Figura 3: Síntese de PRPP. Ribose-5-fosfato é produzida a partir de glicose pela via da pentose-fosfato.

A conversão da ribose-5-fosfato em PRPP é um importante ponto de união entre o metabolismo catabólico da célula e a síntese de uma nova molécula precursora de DNA ou RNA. Neste ponto, o carbono é removido do ciclo das pentoses e comprometido com a síntese de um grande número de metabólitos. PRPP então é necessário para a síntese *de novo* da pirimidina e purina. Embora os produtos imediatos dessas vias sintéticas sejam UMP e IMP, respectivamente, estes compostos são facilmente convertidos em citosina, adenina, guanina e nucleotídeos de uracila e seus derivados 2'-desoxi.

PRPP também é necessário na utilização de bases purinas e pirimidinas exógenas e nucleosídeos. Assim, a reação de PRS é o primeiro passo de uma sequência biossintética altamente ramificada, através do qual uma parcela

substancial de todo o material celular é controlado. Pode-se esperar que tal reação esteja sujeita a um controle metabólico estrito. Switzer e Sogin [31] descreveram que a enzima PRS de alguns organismos é inibida por uma variedade de produtos finais, demonstrando que a PRS de *Salmonella typhimurium* está sob controle repressivo específico mediado pelos nucleotídeos de pirimidina.

Em *M. tuberculosis*, a enzima PRS, de 326 aminoácidos, é codificada pelo gene *prsA* (Rv1017c), possui uma sequência de 981 pares de base, de acordo com a notação do genoma de Mtb H37Rv [32], e apresenta peso molecular aproximadamente 35 kDa.

Esta enzima foi caracterizada em alguns organismos, entre eles: *Salmonella typhimurium* [33], *Escherichia coli* [33], *Bacillus subtilis* [34], *Saccharomyces cerevisiae* [35]. Frequentemente, em eucariotos há mais de um gene *prs*. Na levedura *Saccharomyces cerevisiae* são descritos cinco genes [36]. Já nos humanos, foram identificados os genes de três isoformas de PRS, isoforma 1, variante 1 (**NM_002764.3**), isoforma 2, variante1 (**NM_001039091.2**), isoforma 2, variante 2 (**NM_002765.4**), e isoforma 3 (**NM_175886.2**) expressas em todos os tecidos e no cromossomo X. A isoforma 3 é um gene autossômico expresso especificamente nos testículos. Entre essas três isoformas, há uma identidade de sequência muito elevada (95% entre isoforma 1 e 2; 94% entre isoforma 1 e 3 e 91,2% entre isoforma 2 e 3) [37, 38].

PRS requer o substrato Mg^{2+}·ATP como um grupo doador difosforil; enzimas homólogas de *E. coli* [39], *Salmonella typhimurium* [40] e de mamíferos [41] já foram descritas requerendo também um segundo Mg^{2+} livre

para a sua catálise. A enzima PRS destes organismos, juntamente com *Baccilus subtilis* [42], são representantes da PRS Classe I, possuindo uma estrutura quaternária hexamérica, e uma a inibição alostérica por ADP e GDP [43], a especificidade do substrato ATP como sendo um único grupo doador difosforil, e a dependência pelo fosfato inorgânico (P_i) para a sua atividade [44]. As estruturas tridimensionais de PRS *B. subtilis* (PDB ID: 1IBS) [42] e *Homo sapiens* (PDB ID: 2H06) [37] demonstra que a enzima funcional é um hexâmero de subunidades idênticas, associadas dois a dois, onde cada monômero é composto por dois domínios, ambos com alta similaridade topológica para enzimas da familia fosforribosiltranferase tipo I [45], com aminoácidos conservados [42].

PRS classe II possuem várias características estruturais parecidas com as enzimas da classe I, embora não mostra dependência a íons fosfato e apresenta maior especificidade do substrato, onde GTP, CTP e UTP também podem transferir seus grupos difosforil para a R5P [46]. Até agora, PRS classe II foram identificados apenas em plantas, compreendendo espinafre [47] e homólogos de *Arabidopsis thaliana* [48]. Diferentemente dos PRS homólogos já descritos, o PRS *Methanocaldococcus jannaschii* apresenta uma estrutura quaternária tetramérica (PDB ID: 1U9Y) [46]. Particularmente, o homólogo PRS Archaea é atribuído como pertencente a uma nova PRS classe III [46].

Ao comparar-se a sequência de resíduos de aminoácidos entre a PRS humana e a PRS de Mtb foi observado que a há uma identidade de 41%. No entanto, apesar dessa identidade elevada devem ser levadas em consideração as características cinéticas destas enzimas para que se possa inferir sobre a viabilidade de desenvolvimento de inibidores seletivos. É preciso também

determinar os aminoácidos envolvidos na reação e se são conservados ou não, entre a PRS humana e PRS de Mtb.[49].

1.4 Papel do PRPP

O PRPP tem um importante papel nas diferentes vias metabólicas conforme mostrado na **Figura 3**.

No metabolismo de nucleotídeos participa das duas rotas metabólicas, a via de síntese *de novo* e a via *de salvamento* de nucleotídeos, tanto para purinas como pirimidinas. As vias de síntese *de novo* e *de salvamento* são distintas nos seus mecanismos e em sua regulação, apresentando, no entanto, alguns precursores comuns, como o aminoácido glutamina como fonte de grupamentos amino, e o PRPP derivado da via pentose-fosfato [50].

Na síntese *de novo* de purinas, os nucleotídeos são sintetizados a partir do PRPP. O PRPP é obtido a partir de ribose-5-fosfato, que é produzido a partir de glicose pela via da pentose-fosfato [25], e de ATP, em reação catalisada pela enzima PRS, que é uma enzima regulatória. Na **Figura 4** é mostrada a rota metabólica da biossíntese *de novo* de purinas.

As reações catalisadas pelas enzimas PRS, amidofosforribosil-transferase, adenilossuccinato-sintetase e IMP-desidrogenase são as etapas reguladas da via, sendo que as duas primeiras enzimas controlam a síntese de IMP e as duas últimas controlam a síntese de AMP e GMP, respectivamente.

Um sítio primário de regulação é a síntese de PRPP. A PRS é negativamente afetada por GDP e, em um sítio alostérico distinto, por ADP. Assim, a ligação simultânea de uma oxipurina e uma aminopurina podem ocorrer como resultado sendo uma inibição sinergística da enzima [26].

A maioria das células é capaz de utilizar a via *de salvamento* para a reciclagem de bases livres e nucleosídeos obtidos a partir da dieta ou de outros

tecidos, podendo ser a principal forma de obtenção de nucleotídeos para determinadas linhagens celulares, como os linfócitos [26].

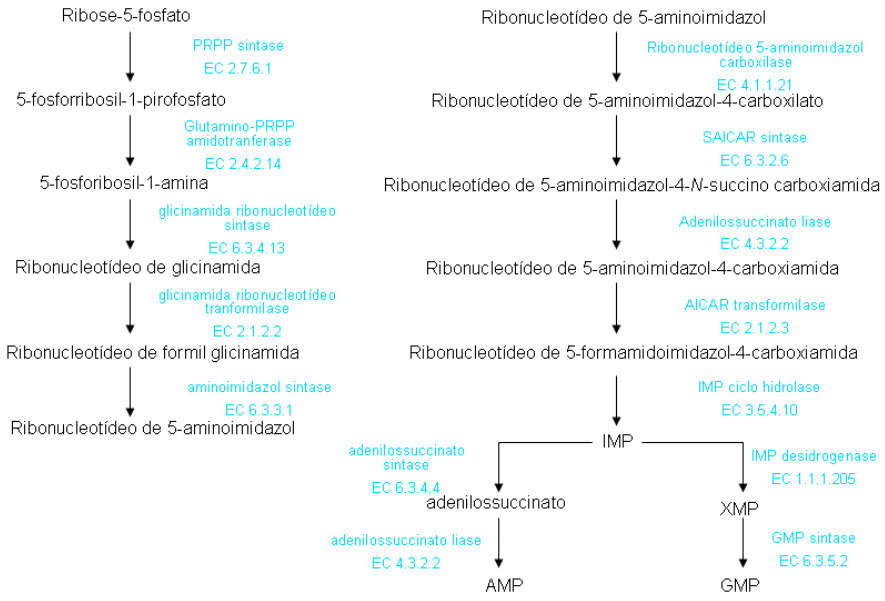

Figura 4: Síntese *de novo* de purinas. A via inicia com a formação de PRPP a partir da ribose-5-fosfato e ATP pela ação da enzima PRS.

As reações da via *de salvamento* permitem que bases livres, nucleosídeos e nucleotídeos sejam facilmente interconvertidos. Guanosina e inosina são convertidos em guanina e hipoxantina, respectivamente, junto com a ribose-1-fosfato, conforme mostra a **Figura 5**. A ribose-1-fosfato pode ser isomerizada a ribose-5-fosfato e, então, a bases livres recuperadas ou degradadas, dependendo das necessidades celulares.

Na síntese dos nucleotídeos pirimídicos, a base nitrogenada é sintetizada primeiro e, então, é ligada à porção ribose-5-fosfato, como mostrado na **Figura 6**.

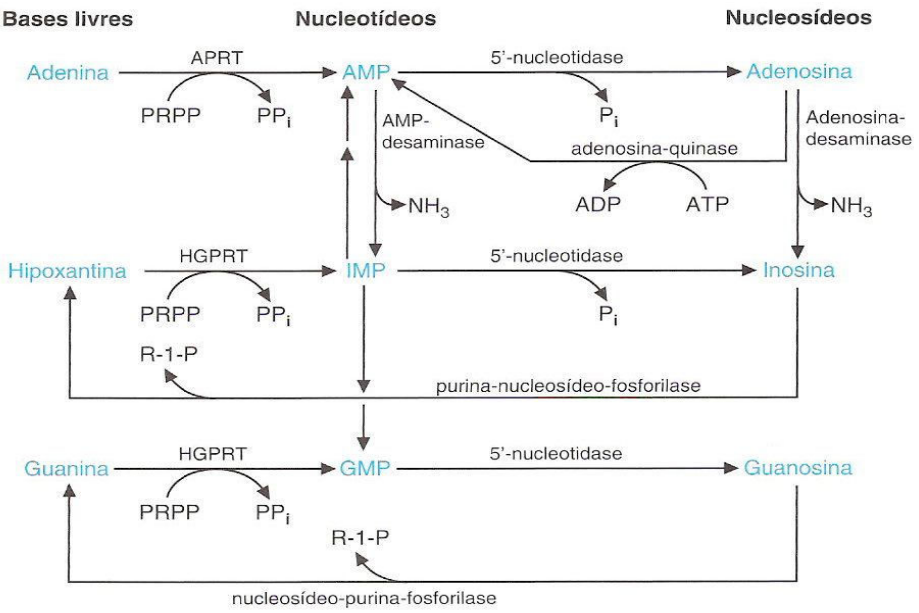

Figura 5: Recuperação de bases. As bases púricas hipoxantina e guanina reagem com PRPP para formar nucleotídeos monofosfato de inosina e monofosfato de guanosina, respectivamente [26].

A via *de novo* começa com a formação de carbamoilfosfato a partir de glutamina, CO_2 e duas moléculas de ATP, em uma reação catalisada pela carbamoilfosfato sintetase II. Uma vez formada a base nitrogenada, a enzima orotato fosforribosiltransferase catalisa a transferência da ribose-5-fosfato a partir PRPP para o orotato, produzindo orotidina-5-fosfato, a qual é descarboxilada pela ácido-orotidílico-desidrogenase para formar monofosfato de uridina UMP. O nucleotídeo UMP pode ser fosforilado a UTP e originar CTP pela adição de um grupamento amina a partir de um aminoácido glutamina [26].

A via *de salvamento* de pirimidinas compreende a conversão direta de bases livre de uracil no seu nucleotídeo correspondente (UMP), pela ação da enzima uracil fosforibosiltransferase, e ainda reações em duas etapas **(Figura 7)**. Assim como na via *de salvamento* de purinas, as reações catalisadas pelas PyNPs são reversíveis, fazendo parte também do catabolismo destes

nucleotídeos. Os nucleosídeos são clivados formando R-1-P e as bases livres citosina, uracil e timina. Citosina é deaminada em uracil e convertida em CO_2, NH_4^+ e β-alanina. Timina é convertida em CO_2 e NH_4^+. [27].

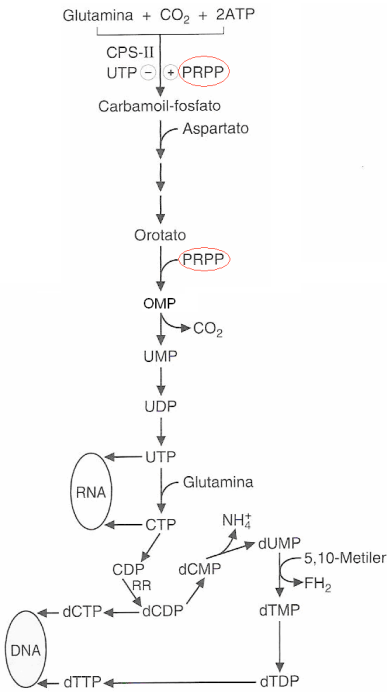

Figura 6: Síntese *de novo* de bases pirimídicas [26].

Além do metabolismo de nucleotídeos o PRPP também participa da biossíntese da histidina e biossíntese do triptofano.

Na biossíntese da histidina, que ocorre em plantas e bactérias, cinco dos seis átomos de carbono da histidina são derivados do PRPP, O sexto carbono da histina origina-se do ATP. Os átomos do ATP que não são incorporados como histidina é eliminado como 5-aminoimidazol-4-carboxila-ribonucleotídeo, que também é um intermediário na biossíntese de purinas [27].

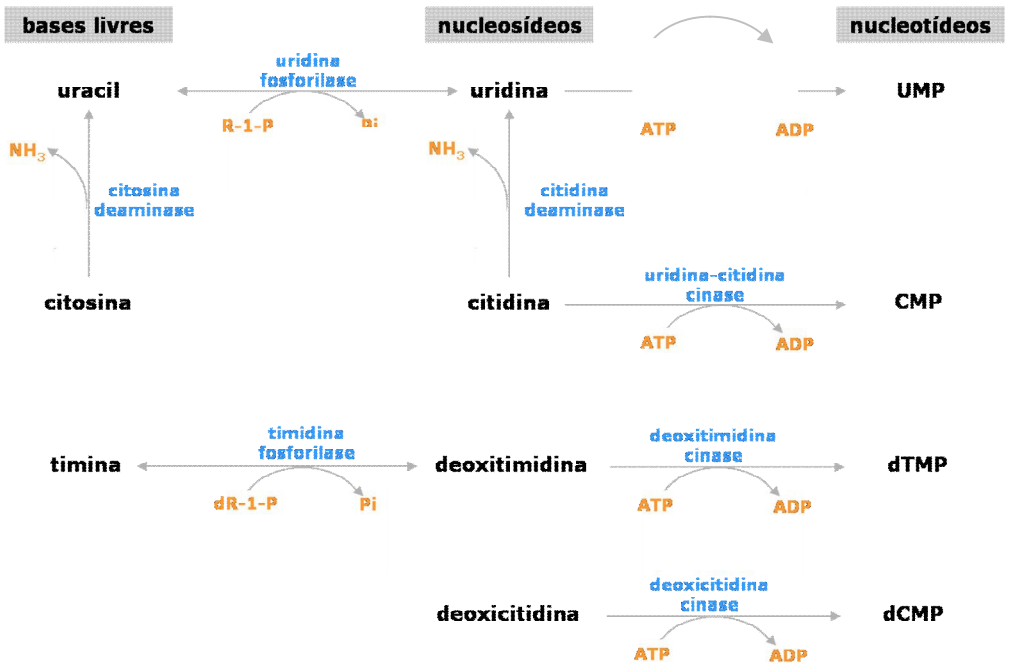

Figura 7. A via *de salvamento* de bases pirimídicas ocorre pela conversão de bases livres em seus respectivos nucleosídeos por pirimidina nucleosídeo fosforilases, seguida pela conversão dos nucleosídeos em nucleotídeos pela ação de nucleosídeo quinases específicas.

Já na biossíntese do triptofano, que é utilizado na síntese de proteínas e no crescimento celular, a via de biossíntese deste aminoácido aromático é de considerável importância devido à sua ausência em animais, existindo apenas em bactérias, fungos e plantas [51]. A síntese do triptofano ocorre a partir de corismato, envolvendo cinco reações catalisadas por enzimas codificadas por um número variável de genes dependendo do microrganismo. O PRPP irá se condensar com o piruvato. Depois de varias etapas ocorre a formação do triptofano. A enzima que catalisa essa reação é a triptofano sintase [27, 51].

2. Objetivos

2.1 Objetivo geral

Caracterização da enzima PRS (EC 2.7.6.1), codificada pelo gene *prsA* de *Mycobacterium tuberculosis* H37Rv como alvo para o desenvolvimento de novas drogas de ação especifica contra o microorganismo *Mycobacterium tuberculosis*, com potencial ação contra as formas ativa e latente da TB.

2.2 Objetivos específicos

i. Amplificação da região codificante para a PRS de Mtb H37RV, através da reação em cadeia da polimerase (PCR);
ii. Clonagem do fragmento amplificado em vetor de expressão procariótico;
iii. Subclonagem em vetor de expressão pET-23a(+);
iv. Sequenciamento e expressão da enzima em diferentes cepas de *Escherichia coli* a fim de obtê-la na forma solúvel;
v. Purificação da proteína recombinante através da técnica de FPLC (*Fast Protein Liquid Cromatography*);
vi. Quantificação total da proteína;
vii. Análise da pureza e identidade da proteína recombinante homogênea por espectrometria de massa e sequenciamento de aminoácidos;
viii. Ensaios de atividade enzimática;
ix. Ensaios de especificidade de substratos;
x. Ensaios de inibição;
xi. Caracterização do mecanismo cinético da enzima, utilizando espectroscopia de fluorescência.

3. Artigo científico submetido à revista PLoS ONE, de índice de impacto 4.4.

"Wild-type Phosphoribosylpyrophosphate Synthase (PRS) from Mycobacterium tuberculosis: a Bacterial Class II PRS?"

Caroline Brancher[a,b,§], Ardala Breda[a,b,§], Leonardo Krás Borges Martinelli[a,b], Cristiano Valim Bizarro[a], Leonardo Astolfi Rosado[a,b], Diógenes S. Santos[a,b*], Luiz A. Basso[a,b*]

[a] Instituto Nacional de Ciência e Tecnologia em Tuberculose (INCT-TB), Centro de Pesquisas em Biologia Molecular e Funcional (CPBMF),

[b]Programa de Pós-Graduação em Biologia Celular e Molecular,

Pontifícia Universidade Católica do Rio Grande do Sul (PUCRS), Av. Ipiranga 6681, Porto Alegre, RS 90619-900, Brazil

[§] Both authors contributed equally to the work.

Wild-type Phosphoribosylpyrophosphate Synthase (PRS) from *Mycobacterium tuberculosis*: a Bacterial Class II PRS?

Caroline B. Borges[a,b,§], Ardala Breda[a,b,§], Leonardo K. B. Martinelli[a,b], Cristiano V. Bizarro[a], Leonardo A. Rosado[a,b], Diógenes S. Santos[a,b*], Luiz A. Basso[a,b*]

[a] Instituto Nacional de Ciência e Tecnologia em Tuberculose (INCT-TB), Centro de Pesquisas em Biologia Molecular e Funcional (CPBMF),

[b]Programa de Pós-Graduação em Biologia Celular e Molecular,

Pontifícia Universidade Católica do Rio Grande do Sul (PUCRS), Av. Ipiranga 6681, Porto Alegre, RS 90619-900, Brazil

[§] Both authors contributed equally to this work.

*Corresponding authors:

Luiz A. Basso

E-mail address: luiz.basso@pucrs.br

Diogenes S. Santos

E-mail address: diogenes@pucrs.br

Av. Ipiranga 6681 – TECNOPUC – Prédio 92A, Porto Alegre, RS 90619-900, Brazil

Phone/Fax: +55 51 33203629

Short title: *M. tuberculosis* PRPP synthase

Abstract

The 5-phospho-α-D-ribose 1-diphosphate (PRPP) metabolite plays essential roles in several biosynthetic pathways, including histidine and tryptophan, nucleotides, and, in mycobacteria, cell wall precursors. PRPP is synthesized from α-D-ribose 5-phosphate (R5P) and ATP by the *Mycobacterium tuberculosis prsA* gene product, phosphoribosylpyrophosphate synthase (*Mt*PRS). Here, we report amplification, cloning, expression and purification of wild-type *Mt*PRS. Glutaraldehyde crosslinking results suggest that *Mt*PRS is a hexamer in solution. *Mt*PRS activity measurements were carried out by a novel coupled continuous spectrophotometric assay. *Mt*PRS enzyme activity could be detected in the absence of inorganic phosphate. ADP and GDP inhibit *Mt*PRS activity. Steady-state kinetics results indicate that *Mt*PRS has broad substrate specificity, being able to accept ATP, GTP, CTP, and UTP as diphosphoryl group donors. Fluorescence spectroscopy data on binary complex formation suggest that the enzyme mechanism of *Mt*PRS for purine diphosphoryl donors follows a random-order of substrate addition and for pyrimidine diphosphoryl donors follows an ordered mechanism of substrate addition in which R5P binds first to free enzyme. An ordered mechanism for product dissociation is followed by *Mt*PRS, in which PRPP is the first product to be released followed by the nucleoside monophosphate products to yield free enzyme for the next round of catalysis. The broad specificity for diphosphoryl group donors and detection of enzyme activity in the absence of P_i would suggest that *Mt*PRS belongs to Class II PRS proteins. On the other hand, the hexameric quaternary structure allosteric inhibition by ADP would place *Mt*PRS in Class I PRSs. Further data are thus needed to classify *Mt*PRS as belonging to a particular family of

PRS proteins. The data here presented should help augment our understanding of *Mt*PRS mode of action. Current efforts are towards experimental structure determination of *Mt*PRS to provide a solid foundation for the rational design of specific inhibitors of this enzyme.

Keywords*: Mycobacterium tuberculosis*; tuberculosis; phosphoribosylpyrophosphate synthase; recombinant protein; PRPP; 5-phospho-α-D-ribose 1-diphosphate; ribose 5-phosphate; enzyme kinetics; enzyme mechanism; fluorescence spectroscopy.

Introduction

Tuberculosis (TB) is a chronic infectious disease caused mainly by *Mycobacterium tuberculosis*, being the second leading cause of mortality by infectious diseases in human populations, killing about 1.7 million people worldwide in 2009 [1]. One third of the world population is estimated to be infected with latent TB. The latter is worsened by the spread of HIV-TB co-infection, which can lead to increased rates of TB reactivation, being up to 30% of deaths among HIV positive subjects caused by the TB bacilli [2]. TB infection is treated by a combination of four drugs that act upon different molecular targets [3]. The treatment regimen includes six month therapy with rifampicin and isoniazid, supplemented with pyrazinamide and ethambutol in the first two months [1]. In recent years, *M. tuberculosis* isolates resistant to one or more of these drugs have been spreading, which seriously hampers the success of measures to control TB [4]. The increasing incidence of TB has been paralleled by a rapid increase of cases caused by multi-drug resistant (MDR-TB) and extensively-drug resistant *M. tuberculosis* strains (XDR-TB), with estimated cases and annual deaths worldwide of, respectively, of 0.5 million and 100,000 for MDR-TB, and 35,000 and 20,000 for XDR-TB [5, 6]. Recently, TB infection with totally resistant strains (TDR-TB) have been described, which are resistant to all first and second line classes of anti-TB drugs tested [7]. There is an urgent need to develop new therapeutic strategies to combat TB. Strategies based on the selection of new targets for antimycobacterial agent development include elucidation of the role played by proteins from biochemical pathways that are essential for mycobacterial growth [8].

Phosphoribosylpyrophosphate synthase (PRS; EC 2.7.6.1) plays central roles in a number of cellular processes, catalyzing the synthesis of 5-phospho-α-D-ribose 1-diphosphate (PRPP; α-D-5-phosphoribosylpyrophosphate; α-D-ribosyl diphosphate 5-phosphate). PRS enzymes catalyze, in the presence of Mg^{2+}, the transfer of β,γ-diphosphoryl moiety of adenosine 5'-triphosphate (ATP) to C1-hydroxyl group of α-D-ribose 5-phosphate (R5P), yielding PRPP [9, 10] (**Figure 1**). PRPP is an essential metabolite for a number of distinct biochemical pathways including *de novo* and salvage pathways of purine and pyrimidine nucleotide synthesis, and biosynthesis of NAD, histidine and tryptophan [11-13]. In Corynebacteriacae, such as mycobacteria, PRPP is a co-substrate for the synthesis of polyprenylphosphate-pentoses, which are the source of arabinosyl residues of arabinogalactan (AG), component of the mycobacterial cell wall, and lipoarabinomannan (LAM), a highly immunogenic lipoglycan that is involved in modulating the host immune response [14, 15].

PRS enzymes usually require Mg^{2+}-ATP as diphosphoryl group donor. The PRS proteins from *Escherichia coli* [16], *Salmonella typhimurium* [17] and mammals [18] have been shown to also require a second free Mg^{2+} ion for increased catalytic rates. PRS enzymes from these organisms, as well as from *Bacillus subtilis* [19], are representative of Class I (also known as "Classical") PRS proteins, with hexameric quaternary structure, allosteric inhibition by purine ribonucleoside diphosphates (adenosine 5'-diphosphate, ADP; and guanosine 5'-diphosphate, GDP), specificity for ATP (or dATP) as diphosphoryl group donor, and requirement of inorganic phosphate (P_i) for enzyme activity [20]. The three-dimensional structures of PRS enzymes from *B. subtilis* (PDB ID: 1IBS) [19] and *Homo sapiens* (PDB ID: 2H06) [10] demonstrate that the functional enzyme is a hexamer of identical subunits, associated two by two, where each monomer is composed by two domains, both

with high topological similarity to the type I phosphoribosyltransferases enzymes family [21]. In addition, there is conservation of amino acid residues in the PRPP substrate binding site [19]. Class II PRS proteins share several structural characteristics with Class I enzymes. However, Class II PRSs are characterized by not being dependent on P_i for activity, have broad specificity for diphosphate donors (including guanosine 5'-triphosphate, GTP; cytosine 5'-triphosphate, CTP; and uridine 5'-triphosphate, UTP), and are not allosterically inhibited by purine ribonucleoside diphosphates [20, 22]. Class II PRS proteins appear to be specific for plants as they have been identified in spinach [23] and *Arabidopsis thaliana* isozymes 3 and 4 [24]. More recently, a PRS enzyme from the archeon *Methanocaldococcus jannaschii* has been shown to be tetrameric (PDB ID: 1U9Y), activated by P_i, non-allosterically inhibited by ADP, and that employs ATP as diphosphate donor [22]. These findings prompted the proposal that *M. jannaschii* PRS belongs to a new Class III of PRPP synthases [22].

Here we describe cloning of *prsA* (Rv1017c) from *M. tuberculosis*; and expression, purification, molecular and kinetic characterization of the non-tagged recombinant PRS (*Mt*PRS). Glutaraldehyde crosslinking results showed that *Mt*PRS is a hexamer in solution. *Mt*PRS activity was assessed by a novel coupled continuous spectrophotometric assay that measures the decrease in orotate catalyzed by *M. tuberculosis* orotate phosphoribosyltransferase in the presence of PRPP formation due to *Mt*PRS enzyme activity. Steady-state data indicate that *Mt*PRS has broad specificity for diphosphoryl group donors and activity in the absence of P_i. These data suggest that *Mt*PRS belongs to Class II PRS family, as plant homologues, even though the primary amino acid structure is indicative of structural resemblance to Class I PRS. To the best of our knowledge, the results

here presented are the first experimental evidence for a bacterial PRS enzyme that can use both pyrimidine and purine nucleosides triphosphates as diphosphoryl group donors. Equilibrium binding data are also presented showing random-order of substrate addition for purine diphosphoryl donors and ordered for pyrimidine diphosphoryl donors, with random-order release of products in which PRPP dissociation is followed by the nucleoside monophosphate products. The *prsA*-encoded protein has been predicted to be essential for *in vitro* growth of *M. tuberculosis* based on transposon-site hybridization studies [25]. More recently, PRS from *Corynebacterium glutamicum*, a model organism used to study *M. tuberculosis* cell physiology, has been shown to be essential for the maintenance of cellular integrity [26]. The results presented here are discussed in light of previous reports on *Mt*PRS [26, 27], and thus contribute to a better understanding of *Mt*PRS. As *Mt*PRS shares a significant degree of identity with human PRS, elucidation of the mode of action of the former should provide a basis on which to design species-specific inhibitors to be tested as anti-TB agents. It is also hoped that the biochemical data here presented may contribute to functional genomic efforts. Understanding the mode of action of *Mt*PRS may be useful to chemical biologists interested in designing function-based chemical compounds to elucidate the biological role of this enzyme in the context of whole *M. tuberculosis* cells, including active and latent stages of infection [15, 28].

Methods

Gene amplification

The *prsA* gene (Rv1017c) was PCR amplified from total genomic DNA of *M. tuberculosis* H37Rv strain using specific primers designed to contain *Nde*I (primer sense 5'GCCATATGAGCCACGACTGGACCGATAATCG3') and *Bam*HI (primer antisense 5'GCGGATCCTCATGCGTCCCCGTCGAAAAGT3') restriction sites (underlined). An internal restriction site for *Nde*I was removed from the gene sequence by site-directed mutagenesis at codon position 170, in which a thymine was replaced with a cytosine at codon's third position (CAT to CAC), resulting in a sense mutation that maintained a histidine amino acid at this position. PCR cycling parameters were as follows: an initial denaturation step at 96°C for 5 min, 35 cycles of denaturation at 96°C (30 sec), annealing at 60°C (1 min 30 sec) and extension at 72°C (2 min 30 sec) and a final extension step for 10 min at 72° C. Dimethyl sulfoxide (DMSO) was added to the PCR reaction at final concentration of 10%. The PCR product was visualized on 1% agarose gel and purified from the gel utilizing the Quick Gel Extraction kit (Invitrogen). The purified fragment was initially cloned into pCR-Blunt® vector (Invitrogen) and subcloned into pET-23a(+) expression vector (Novagen). The latter was previously digested with *Nde*I and *Bam*HI restriction enzymes. The integrity of constructs was confirmed in all cases by appropriate selections and digests with appropriated restriction enzymes (New England Biolabs). Inserted sequences were confirmed by DNA sequencing in all cases.

Expression of recombinant MtPRS

Competent *E. coli* BL21(DE3) (Novagen) cells were electroporated with pET-23a(+)::*prsA* recombinant vector and selected on Luria-Bertani (LB) agar plates containing 50 µg mL^{-1} ampicillin. A single colony was used to inoculate 50 mL of LB medium containing 50 µg mL^{-1} ampicillin and grown overnight at 37ºC. Aliquots of

cell culture (5 mL) were used to inoculate 500 mL of Terrific Broth (TB) medium in 4 x 2 L flasks supplemented with ampicillin (50 µg mL^{-1}), grown at 37°C and 180 rpm to an optical density (OD_{600nm}) of 0.4 – 0.6. At this growth stage, culture temperature was lowered to 30ºC and protein expression was carried out without isopropyl-β-D-thiogalactopyranoside (IPTG) induction, for 24 hours. Cells were harvested by centrifugation (11,800 *g*) for 30 min at 4°C and stored at -20ºC. Expression of the recombinant protein was confirmed by 12% sodium dodecyl sulfate polyacrylamide gel electrophoresis (SDS-PAGE) stained with Coomassie Brilliant Blue [29].

Purification of recombinant MtPRS

All protein purification steps were performed at 4°C or on ice. Chromatographic steps were performed by High-Performance Liquid Chromatography (HPLC) on Äkta Purifier System (GE HealthCare). Cell pellet (4 g) was suspended in 40 mL of buffer A (Tris-HCl 50 mM pH 7.5) and stirred for 30 min. Lysozyme (Sigma Aldrich) was added to a final concentration of 0.2 mg mL^{-1} and incubated for 30 min at constant stirring. The mixture was sonicated (10 pulses of 10 sec, with intervals of 1 min off), and cell debris were removed by centrifugation at 48,000 *g* for 30 min. Streptomycin sulfate (Sigma-Aldrich) was added to the supernatant to a final concentration of 1% (wt/vol), stirred for 30 min, and centrifuged at 48,000 *g* for 30 min. The supernatant was treated with ammonium sulfate at a final 2.5 M concentration, stirred for 30 min and pelleted by centrifugation at 48,000 *g* for 30 min. The resulting supernatant fraction at this step was discarded and the precipitate was suspended in 40 mL of buffer A (crude extract). The crude extract was loaded on a Q-Sepharose Fast Flow anion exchange column (GE Healthcare) equilibrated with buffer A. The column was washed with 5 column volumes (CV) of

buffer A and the adsorbed material was eluted with 20 CV of 0-100% linear gradient of Tris-HCl 50 mM NaCl 0.5 M pH 7.5 (buffer B) at 1 mL min^{-1} flow rate. Fractions containing *Mt*PRS, as inferred by 12% SDS-PAGE polyacrylamide gel electrophoresis stained with Coomassie Brilliant Blue [29], were pooled and concentrated to 7 mL using a 50 mL stirred ultrafiltration cell (Millipore) with 10 kDa cutoff filter. The sample was loaded on a Superdex 200 size exclusion column (GE Healthcare) previously equilibrated with buffer A. Proteins were eluted in isocratic conditions with 1 CV of buffer A at 0.5 mL min^{-1} flow rate. Eluted fractions containing homogeneous *Mt*PRS were concentrated using 50 mL stirred ultrafiltration cell (Millipore) with 10 kDa cutoff filter to a final concentration of 0.36 mg mL^{-1} and stored at -80 ºC. Total protein concentration was determined by Bradford's method using bovine serum albumin as standard (Bio-Rad Laboratories) [30].

MtPRS identification by mass spectrometry

*Protein desalting***.** Purified *Mt*PRS samples were desalted with a reverse chromatography phase (POROS R2-50 resin, Applied Biosystems) using lab-made columns built with glass fiber in 200 µL pipette tips. The columns were activated with methanol and equilibrated with 0.046% trifluoroacetic acid (TFA) previous to sample loading. Samples were washed twice with 0.046% TFA and eluted with 80% acetonitrile/0.046% TFA, and dried using a SpeedVac concentrator (Thermo Scientific).

*Trypsin digestion***.** The in-solution trypsin digestion of *Mt*PRS was performed using a protocol adapted from [31]. Desalted and dried samples of *Mt*PRS containing 35 µg of protein (1 nmol) were ressuspended in 50 µL of 0.1% (w/v) RapiGest SF (Waters Corp.) acid labile surfactant diluted in 50 mM Ammonium Bicarbonate, pH

7.8. The samples were heated to 99℃ for 2 min and dithiothreitol (DTT) was added to a final concentration of 5 mM. After incubation at 60 ℃ for 30 min, iodoacetamide was added to a final concentration of 15 mM and the samples were maintained at room temperature for 30 min protected from light. Trypsin enzyme was added at 1:100 enzyme/protein ratio in the presence of $CaCl_2$ at 1mM final concentration, and incubated for 1 h at 37 ℃. For surfactant degradation, HCl was added at a final concentration of 100 mM. The samples were centrifuged at 14,000 rpm for 10 min at 4℃, and the supernatants were transferred to clean tubes.

LC-MS/MS peptide mapping experiments. Chromatographic separations of digested peptide mixtures were performed using a nanoLC Ultra system (nanoLC Ultra 1D plus, Eksigent, USA) equipped with a nanoLC AS-2 autosampler (Eksigent, USA). The nanoflow system was connected to a LTQ-Orbitrap hybrid mass spectrometer (LTQ-XL and LTQ Orbitrap Discovery, Thermo Electron Corporation, San Jose, CA) equipped with a Finnigan™ nanospray ionization (NSI) source (Thermo Electron Corporation, San Jose, CA). Separation of digested samples was performed with 15 cm capillary columns (150 µm i.d.) packed in-home with Kinetex 2.6 µm C18 core-shell particles (Phenomenex, Inc.) using a slurry packing procedure [32]. The chromatographic method used a flow rate of 300 nL/min with a step gradient from mobile phase A containing 0.1% formic acid in water to mobile phase B containing 0.1% formic acid in acetonitrile (0-2% B over 5 min; 2-10% B over 3 min; 10-60% B over 60 min; 60-80% B over 2 min; 80% B isocratic for 10 min; 80-2% B over 2 min; and 2% B isocratic for 8 min). The nano-ESI infusion was performed using the NSI-1 dynamic nanospray probe (Thermo Scientific, Inc.) equipped with a silica-tip emitter of 10 µm diameter tip (PicoTip, New Objective, Inc., Woburn, MA, USA). Spectra of eluting peptides were acquired in positive ion mode in a data-

dependent fashion. First, the instrument was set to acquire one MS survey scan for the m/z range of 400-2000 with resolution of 30,000 (at m/z 400) followed by MS/MS spectra of the five most intense ions from each survey scan. MS/MS fragmentation was performed using collision-induced dissociation (CID) with an activation Q of 0.250, an activation time of 30.0 ms, 35% of normalized collision energy, and an isolation width of 1.0 Da. To detect low intensity ions, we employed a dynamic exclusion of ions lasting for 30 sec during acquisition of MS/MS spectra. LC-MS/MS data were compared with theoretical MS/MS spectra obtained from *in-silico* tryptic digests of the *M. tuberculosis* H37Rv proteome (ftp://ftp.ncbi.nih.gov/genomes). We allowed two missed cleavage sites for trypsin, a precursor tolerance of 10 ppm, a fragment tolerance of 0.8 Da, static carbamidomethylation of cysteine residues, and oxidation of methionine residues. To reduce false identifications, data analysis was restricted to matches with Xcorr score > 2.0 for doubly charged ions and Xcorr score > 2.5 for triply charged ions.

Determination of MtPRS molecular mass. Purified *Mt*PRS samples were desalted, reconstituted in acetonitrile 50%/formic acid 0.1% and directly injected using a 500 µL syringe (Hamilton Company, USA) in a static mode into an IonMax electrospray ion source. The electrospray source parameters were as follows: positive ion mode, 5 kV of applied voltage to the electrospray source, 5 arbitrary units (range 0-100) of sheath gas flow, 31.7 V of capillary voltage, 285 °C of capillary temperature, and 159 V of tube lens voltage. Full spectra (600 – 2000 m/z range) were collected during 10 min on a Thermo Orbitrap Discovery XL in profile mode at a nominal resolution r = 30,000 at m/z 400 using FT automatic gain control target value of 1,000,000 charges. The average spectrum was processed with the software MagTran [33] for charge state deconvolution.

MtPRS quaternary structure assessment by cross-linking studies

Cross-linking studies of the protein's oligomeric state were performed as described elsewhere [34], in standard 24 well plates. Each plate reservoir was loaded with 120 µL of 25% v/v glutaraldehyde acidified with 3 µL HCl 5 N. A coverslip containing 15 µL drop of protein suspension (0.36 mg mL^{-1} homogeneous recombinant *Mt*PRS in buffer A) was used to seal the reservoir. The plate was incubated at 30ºC for different time intervals (10, 20, 30, 40 min). Protein drops were collected at the end of each incubation time and subsequently analyzed by 12% SDS-PAGE.

Enzyme activity assay of recombinant MtPRS

All chemicals in enzyme activity measurements were purchased from Sigma Aldrich. *Mt*PRS activity was measured by a coupled continuous spectrophotometric assay in quartz cuvettes using a UV-visible Shimadzu spectrophotometer UV2550 equipped with a temperature-controlled cuvette holder. *Mt*PRS PRPP synthesis (ATP + R5P → PRPP + AMP) was coupled to *M. tuberculosis* orotate phosphoribosyltransferase (*Mt*OPRT, EC 2.4.2.10) forward reaction (OA + PRPP → OMP + PP_i), monitoring the decrease in orotate (OA) concentration. Homogeneous recombinant *Mt*OPRT was obtained as to be described elsewhere [A. Breda, L.A. Rosado, D.M. Lorenzini, L.A. Basso, and D. S. Santos, manuscript submitted for publication in Molecular BioSystems]. The reaction mixture (500 µL) contained Tris-HCl 50 mM $MgCl_2$ 20 mM pH 8.0, OA 100 µM, *Mt*OPRT 1.3 µM, and varied concentrations of ATP and R5P, in either absence or presence of varied P_i

concentrations. Enzyme reaction was started by addition of *Mt*PRS, and the linear decrease in absorbance at 295 nm upon OA → OMP conversion was followed for 60 sec at 25°C, using an extinction coefficient value of 3950 $M^{-1}cm^{-1}$ [35]. One unit of *Mt*PRS is defined as the amount of enzyme necessary to convert 1 µmol of R5P to PRPP per min in an optical path of 1 cm. All enzyme activity assays were performed in triplicate.

Substrate specificity assay

To evaluate whether *Mt*PRS is able to use purine or pyrimidine nucleotides other than ATP as diphosphoryl group donor, enzyme activity was monitored as described above, at fixed R5P (50 µM) and *Mt*PRS (10 µM) concentrations, replacing ATP with CTP, GTP or UTP, at 10 to 30 µM range. Effects of CTP, GTP and UTP on the *Mt*PRS-catalyzed chemical reaction were compared to ATP at varying concentrations (10 to 60 µM) under the same assay conditions.

Inhibition assay

Inhibition assays were performed at fixed R5P (50 µM), ATP (60 µM), and *Mt*PRS (10 µM) concentrations, in either absence or presence of varied concentrations of ADP and GDP (10 µM to 20 mM). Activity measured in the absence of ADP and/or GDP was considered to be 100%, and inhibitory effect for each dinucleotide was calculated as a function of percentage or residual *Mt*PRS enzyme activity on inhibitor concentration. All measurements were performed in duplicate or triplicate with at least five dinucleotide concentrations. The IC_{50} value (concentration of inhibitor required to reduce the fractional enzyme activity to half of its initial value in the absence of inhibitor) was obtained from fitting the data to either

Eq. (1) for complete inhibition or to **Eq. (2)** for partial inhibition [36]. For **Eq. (1)** and **(2)**, v_0 is the enzyme activity in the absence of inhibitor, and v_i represents the fractional enzyme activity in the presence of inhibitor at [I] concentration [36]. For **Eq. (2)**, $v_{i(max)}$ is the maximum value observed for the residual enzyme activity in the absence of inhibitor (corresponding to v_0), and $v_{i(min)}$ represents the minimum residual enzyme activity value in the presence of high inhibitor concentrations [36].

$$\frac{v_i}{v_0} x100 = \frac{100}{1 + \frac{[I]}{IC_{50}}} \qquad \textbf{Eq. (1)}$$

$$\frac{v_i}{v_0} x100 = \frac{\left(\frac{v_{i(\max)}}{v_0} - \frac{v_{i(\min)}}{v_0} \right) x100}{1 + \frac{[I]}{IC_{50}}} + \frac{v_{i(\min)}}{v_0} x100 \qquad \textbf{Eq. (2)}$$

Primary amino acid sequence analysis

Amino acid sequence alignment of PRS homologues was derived from nucleotides multi sequence neighbor-joining alignment performed with MEGA 5 software [37], using software's default parameters. Nucleotides sequences were obtained from GenBank database for *Homo sapiens* PRS isoform 1, variant 1 (**NM_002764.3**), isoform 2, variant 1 (**NM_001039091.2**), isoform 2, variant 2 (**NM_002765.4**), and isoform 3 (**NM_175886.2**), also known as isoform 1-like. PRS coding DNA sequences for *Arabidopsis thaliana* isoform 1 (**X83764**), isoform 2 (**X92974**), isoform 3 (**AJ012406**), isoform 4 (**AJ012407**), and *Spinacia oleracea* isoform 1 (**AJ006940**), isoform 2 (**AJ006941**), isoform 3 (**AJ006942**), and isoform 4 (**AJ006943**) were available on EMBL. Nucleotide sequence for *M. tuberculosis prsA*

gene was obtained from TubercuList database (http://genolist.pasteur.fr/TubercuList/). Human PRS isoform 1, variant 2 was excluded from alignment as it presents a short nucleotide length (345 base pairs, coding for an abortive 115 amino acids long polypeptide).

Fluorescence spectroscopy

Fluorescence titration was carried out to assess binary complex formation at equilibrium between *Mt*PRS and either substrate(s) or product(s) at 25°C. All substrates (R5P, ATP, GTP, UTP and CTP), products (AMP and PRPP) and the enzyme were dissolved in Tris HCl 50 mM pH 7.5 containing $MgCl_2$ 20 mM. Fluorescence titration with R5P was performed by making microliter additions of 1 mM and 4 mM R5P (0.99 – 126.83 µM final concentrations) to 1 mL of 3 µM *Mt*PRS, keeping the dilution to a maximum of 5.6%. Fluorescence titration with ATP was performed by making microliter additions of 1 mM, 4 mM and 10 mM ATP (0.9 – 169.65 µM final concentrations) to 1mL of 3 µM *Mt*PRS, keeping the dilution to a maximum of 3.8%. Fluorescence titration with GTP was performed by making microliter additions of 1 mM, 4 mM and 10 mM GTP (0.9 – 309.24 µM final concentrations) to 1 mL of 3 µM *Mt*PRS, keeping the dilution to a maximum of 5.2%. Fluorescence titration with UTP was performed by making microliter additions of 1 mM, 4 mM and 10 mM UTP (0.9 – 389.25 µM final concentrations) to 1mL of 3µM *Mt*PRS, keeping the dilution to a maximum of 5%. Fluorescence titration with CTP was performed by making microliter additions of 1 mM, 4 mM and 10 mM CTP (0.9 – 389.25 µM final concentration) to 1mL of 3 µM *Mt*PRS, keeping the dilution to a maximum of 5%. Fluorescence titration with AMP was performed by making microliter additions of 1mM, 4 mM and 10 mM AMP (0.99 – 389.25 µM final

concentrations) to 1 mL of 3 µM *Mt*PRS, keeping the dilution to a maximum of 5% Fluorescence titration with PRPP was performed by making microliter additions of 1mM and 4 mM PRPP (0.99 – 389.25 µM final concentrations) to 1 mL of 3.0 µM *Mt*PRS, keeping the dilution to a maximum of 5%. Measurements of intrinsic protein fluorescence of *Mt*PRS employed excitation wavelength values of 292 nm (R5P) and 295 nm (PRPP, AMP, ATP, GTP, UTP and CTP), and the emission wavelength ranged from 300 nm to 400 nm (maximum *Mt*PRS λ_{EM}=336 nm). In the binding experiments, different slits for the excitation and emission wavelengths were employed, 1.5 nm and 5 nm for R5P respectively, 1.5 nm and 10 nm for binding of ATP, GTP, UTP and CTP, and also 1.5 nm and 10 nm for the products AMP and PRPP. Control experiments were performed in the same conditions, in the absence of *Mt*PRS, and the values found in the control experiments were subtracted from those obtained in the presence of the enzyme. Data from equilibrium fluorescence spectroscopy were fitted to **Eq. (3)** for hyperbolic binding isotherms, in which K represents the dissociation constant for binding of substrate and/or product to *Mt*PRS (K_D). Sigmoidal binding data were fitted **Eq. (4)**, the Hill equation [38], in which F is the observed fluorescence signal, F_{max} is the maximal fluorescence intensity, n represents the number of substrate binding sites for high cooperativity (or the Hill coefficient that is indicative of cooperative index), and K' is a constant comprising interaction factors and the intrinsic dissociation constant [39].

$$v = \frac{VA}{K + S} \qquad \textbf{Eq. (3)}$$

$$\frac{F}{F_{max}} = \frac{A^n}{K' + A^n} \qquad \textbf{Eq. (4)}$$

Results

Cloning, expression and purification of recombinant MtPRS

A PCR amplification product consistent with the expected size for the *M. tuberculosis prsA* (981 bp) coding sequence was detected by 1% agarose gel electrophoresis (data not shown). This amplicon was purified and cloned into the pET-23a(+) expression vector. Automated DNA sequencing confirmed the identity of the insert and absence of mutations in the pET-23a(+)::*prsA* construct. SDS-PAGE (12%) analysis indicated that the best experimental conditions for expression of recombinant *Mt*PRS in the soluble fraction in *E. coli* BL21(DE3) host cells were as follows: TB medium, cell growth at 37°C up to an OD_{600nm} of 0.4 – 0.6, no IPTG induction, followed by cell growth for 24 hours at 30°C (data not shown). SDS-PAGE analysis was based on detection of a protein band with expected apparent subunit molecular mass of ~35 kDa, which is in agreement with the predicted molecular mass (35,459.3 Da).

Recombinant *Mt*PRS protein was purified to homogeneity (**Figure 2**) by a two-step chromatographic protocol, with 9.3% yield and 10 fold purification (**Table 1**). Cell pellet of host cells were treated with lysozyme, sonicated, treated with streptomycin sulfate, ammonium sulfate and centrifuged as described in the Methods section. The pellet was suspended in buffer A (this suspension is referred to as crude extract on Table 1), loaded on a Q-Sepharose Fast Flow anion exchange column, and recombinant *Mt*PRS protein desorption occurred at approximately 390 mM salt concentration. This anion exchange step removed substantial amount of contaminants from the protein sample. The fractions containing *Mt*PRS were pooled, loaded on Superdex 200 size exclusion column, and isocratic elution yielded

homogeneous protein with concomitant salt removal. This apparently homogeneous recombinant *Mt*PRS protein preparation (0.36 mg mL^{-1} in buffer A) was stored at -80ºC with no apparent loss of activity for 7 months.

Mass spectrometry analyses

LC-MS/MS peptide mapping experiments. Apparently homogeneous *Mt*PRS samples were desalted, digested with trypsin, and the peptide mixtures subjected to LC-MS/MS analysis (see Methods). 188 spectra were obtained and identified with 27 different peptides derived from the trypsin digestion of the *Mt*PRS protein. These peptides covered 61% of the *Mt*PRS sequence.

Molecular mass determination by mass spectrometry. The spectra of intact *Mt*PRS samples were recorded with the Orbitrap analyzer for molecular mass determination (see Methods). Peaks corresponding to different charge states spanning from 29^+ to the multiple charge state 54^+ were detected. From the deconvoluted spectra, a value of 35,345 Da was determined for the average molecular mass of *Mt*PRS, consistent with the post-translational removal of the N-terminal methionine (theoretical subunit molecular mass = 35,477.47 Da) (**Figure 3**).

MtPRS quaternary structure assignment

*Mt*PRS molecular mass could not be assigned by analytical HPLC gel filtration chromatography due to formation of protein aggregates under the experimental conditions described elsewhere [40]. Cross-linking experiments were thus pursued. The homogeneous *Mt*PRS was incubated with glutaraldehyde for several time intervals prior to 12% SDS–PAGE analysis [34]. This analysis indicates that the enzyme quaternary structure correspond to a hexamer of identical subunits, as

Coomassie Brilliant Blue stained gel presented two main bands corresponding to the expected molecular mass for monomeric (35 kDa) and hexameric (210 kDa) *Mt*PRS, in which there appears to be a shift from monomeric to hexameric state over incubation time (**Figure 4**). After 10 min incubation time, multi oligomeric *Mt*PRS states can be visualized, corresponding to weaker stained bands (approximately 70 kDa – dimer, 120 kDa – trimer, and 150 kDa – tetramer). These intermediate oligomeric states are converted to the predominant hexameric form over incubation time (**Figure 4**, lane 7). Lane 1 corresponds to monomeric (55 kDa) and tetrameric (219 kDa) oligomers of inosine monophosphate dehydrogenase (IMPDH, EC 1.1.1.205) from *M. tuberculosis* [D.C. Rostirolla, T.M. Assunção, L.A. Basso, D.S. Santos, manuscript in preparation].

Enzyme activity, substrate specificity, inhibition assays and dependence of MtPRS on P_i

*Mt*PRS activity could be measured in a coupled assay with *Mt*OPRT, in which the PRPP product of *Mt*PRS enzyme activity serves as substrate for *Mt*OPRT which, in the presence of OA, yields orotidine 5'-monophosphate (OMP) and pyrophosphate (PP_i). *Mt*PRS activity can thus be monitored by measuring the decrease in absorbance at 295 nm upon conversion of OA to OMP. *Mt*PRS enzyme activity could be detected in the absence of P_i, and in the presence of varying concentrations of Mg^{2+}-ATP diphosphoryl group donor and fixed concentration of R5P at 50 µM (**Figure 5A**). Interestingly, addition of 10-50 mM of P_i to the assay mixtures abrogated *Mt*PRS enzyme activity.

*Mt*PRS enzyme activity could be detected when, under the same experimental conditions, the Mg^{2+}-ATP diphosphoryl group donor was replaced with either other

purine (GTP) or pyrimidine (CTP and UTP) nucleoside 5'-triphosphates (**Figure 5B**). These results indicate that *Mt*PRS has broad substrate specificity, being able to use Mg^{2+}-ATP, Mg^{2+}-GTP, Mg^{2+}-CTP, and Mg^{2+}-UTP as diphosphoryl group donors.

Addition of both ADP (**Figure 6A**) and GDP (**Figure 6B**) to *Mt*PRS standard assay (ATP and R5P fixed at 60 µM and 50 µM, respectively, in an assay mixture containing *Mt*PRS 10 µM, OA 100 µM, *Mt*OPRT 1.3 µM, and $MgCl_2$ 20 mM, Tris HCl 50 mM, pH 8.0) resulted in inhibition of enzyme activity. The data on partial enzyme inhibition by ADP (**Figure 6A**) were fitted to **Eq. (2)**, yielding an IC_{50} value of 802 (± 178) µM. The data on complete enzyme inhibition by GDP **(Figure 6B)** were fitted to **Eq. (1)**, yielding an IC_{50} value of 86 (± 7) µM.

To ascertain whether or not these experimental data were due to effects specifically on *Mt*PRS activity and not on *Mt*OPRT coupled enzyme, measurements of the latter enzyme were performed in the presence of the diphosphoryl group donors (ATP, GTP, CTP, and UTP), nucleoside diphosphate inhibitors (ADP and GDP), and P_i. The presence of any of these molecules in the assay mixtures employed in the coupled assays (OA 100 µM, *Mt*OPRT 1.3 µM, $MgCl_2$ 20mM, containing PRPP 500 µM) did not have any effect on *Mt*OPRT enzyme activity to any extent (data not shown). Accordingly, the effects of the alternative diphosphoryl group donors, nucleoside 5'-diphosphate inhibitors and P_i were solely due to changes in *Mt*PRS enzyme activity.

Fluorescence spectroscopy

Binary complex formation between either substrate(s) or product(s) and *Mt*PRS was assessed by equilibrium fluorescence spectroscopy to ascertain the order of, or lack of, addition of these chemical compounds. The binary complex

formation of binding of either R5P, ATP, GTP (an alternative diphosphoryl group donor), or AMP upon *Mt*PRS resulted in a quench in protein fluorescence. Titration of *Mt*PRS with R5P (**Figure 7A**), ATP (**Figure 8A**), and GTP (**Figure 8B**) were hyperbolical. These data were thus fitted to **Eq. (3)**, yielding K_D values of 61 (± 3) μM for R5P, 18 (± 2) μM for ATP, and 21 (± 2) μM for GTP. The K_D value is the overall dissociation constant for the binary complex formation between the enzyme and either substrate or product. Titration of *Mt*PRS with AMP product was sigmoidal (**Figure 7B**), and fitting the data to **Eq. (2)** (the Hill equation) yielded a value of 109 (± 3) μM for *K'*. The *K'* value is a mean dissociation constant for the binary complex formation between the enzyme and the product AMP, which is comprised of the intrinsic dissociation constant and interactions factors [39]. There was no intrinsic protein fluorescence change upon binding of PRPP product to *Mt*PRS, suggesting that PRPP cannot bind to free enzyme. Binding experiments were also carried out in an attempt to determine whether or not there is binary complex formation between *Mt*PRS and the alternative substrates GTP, UTP and CTP, which can substitute for ATP as diphosphoryl group donors. No change in protein fluorescence could be detected upon binding of UTP and CTP (alternative diphosphoryl group donors having pyrimidine bases) to *Mt*PRS, suggesting that neither could bind to free enzyme. Interestingly, binding of the alternative diphosphoryl group donor having a purine base (GTP) could be detected (**Figure 8B**).

Discussion

The PCR product consistent with the expected size for the *M. tuberculosis prsA* (981 bp) coding sequence was cloned into the pET-23a(+) expression vector,

and automated DNA sequencing confirmed both identity and absence of mutations in the pET-23a(+)::*prsA* construct. Interestingly, expression in *E. coli* BL21(DE3) host cells was achieved in the absence of IPTG induction (data not shown). In the pET vector system (Novagen), target genes are positioned downstream of bacteriophage T7 late promoter [41]. High levels of protein expression even in the absence of IPTG inducer have been shown to occur in the pET system when cells approach stationary phase in complex medium, which may be part of the general cellular response to nutrition limitation [42]. However, more recently, it has been shown that unintended induction in the pET system is due to the presence of as little as 0.0001% of lactose in the medium [43].

Recently, Alderwick and co-workers [26] and Lucarelli and co-workers [27] have reported cloning and purification of His-tagged *Mt*PRS. The protocols for cloning and purification of recombinant protein are significantly different from the ones previously reported [26, 27], since *Mt*PRS reported here was produced as a non-His-tagged protein. Although many protocols use histidine tags to facilitate protein purification by the nickel-affinity chromatography strategy, adding histidine tags may alter the protein structure and the biological activity [44, 45]. We have thus deemed appropriate to make efforts to produce recombinant *Mtb*PRS without any fusion partner to avoid any possible effect that the latter may have on the former. Notwithstanding, it should be pointed out that steady-state kinetics results were shown by others to be quite similar for His-tagged *Mt*PRS as compared to *Mt*PRS treated with protease for removal of the N-terminal His-tag fusion partner [27]. The two-step chromatographic purification protocol of recombinant *Mt*PRS here described yielded 2.6 mg of homogenous protein from 4 g of wet cell paste (**Figure 2** and **Table 1**). Recombinant *Mt*PRS protein was stable at -80ºC in the absence of

additives. However, homogeneous *Mt*PRS could not be concentrated above 1 mg mL^{-1} in Tris HCl 50mM pH 7.8 without precipitation, and activity of precipitated protein could not be recovered. Interestingly, Alderwick and co-workers [26] showed that recombinant C-terminal His-tagged *Mt*PRS was stable in solution up to 2 mg mL^{-1} in KH_2PO4 buffer at pH 7.9 containing 150 mM NaCl, 1mM DTT, 10% glycerol. It has been reported that addition of ammonium sulfate or Mg^{2+}-ATP was needed to preserve 20% of *Mt*PRS activity and full activity could be maintained with addition of inorganic phosphate [27]. No loss of activity could be observed for *Mt*PRS in Tris HCl 50 mM pH 7.5 buffer for the protein preparation here described. The possible explanations for these conflicting experimental observations are rather elusive at the moment.

Three different classes of PRP enzymes have been described so far. Classifications of PRS proteins as belonging to Class I (also known as “Classical”), Class II or Class III are based on specificity for diphosphoryl donors, requirement of P_i for activity, allosteric inhibition by purine ribonucleoside diphosphates, and oligomeric states [20, 22, 27]. PRS enzymes from *E. coli* [16], *S. typhimurium* [17], *B. subtilis* [19], and human isoform 1 [10] are representative of Class I, with hexameric quaternary structure, allosteric inhibition by ADP and GDP, specificity for ATP or dATP as diphosphoryl donor, and requirement of P_i for activity. Class II PRSs, which appear to be specific for plants, are trimeric, not allosterically inhibited by purine ribonucleoside diphosphates, have broad specificity for diphosphoryl group donors (including GTP, CTP, and UTP), and not dependent on P_i for activity [20, 22]. The Class III PRS from *M. jannaschii* has been shown to be tetrameric, activated by P_i, non-allosterically inhibited by ADP (it probably binds to ATP active site), and that employs ATP and dATP as diphosphate donors [22]. It has been proposed that there

is a proportional relationship among K_M, V_{max} and PRS classes [22], in which Class III enzymes have larger K_M values for R5P and ATP substrates, Class I with de lowest values, and Class II with intermediate values [22]. The extent to which these criteria could be used for classifying PRS enzymes are still not clear due to limited number of representatives of Classes II and III PRSs [22].

*Mt*PRS quaternary structure could not be unequivocally determined by size exclusion liquid chromatography, in agreement with previous reports on PRS enzymes showing a tendency of these proteins to exist in multiple aggregated states in solution, ranging from dimeric to octameric quaternary structures [46, 47]. Accordingly, the glutaraldehyde cross-linking method followed by SDS-PAGE analysis [34] were employed to assess the oligomerization state of *Mt*PRS in solution. These results suggest that recombinant *Mt*PRS is a hexamer in solution (**Figure 4**), for the observed SDS-PAGE bands consistent with molecular mass values of 35 kDa and 210 kDa correspond to the enzyme's monomeric and hexameric states, respectively. The subunit molecular mass determined from LC/MS experiments indicated a subunit molecular mass value of 35,345 Da (**Figure 3**). Quaternary structure assignment of PRS enzymes in solution is still ambiguous, with varying results in presence and absence of ligands [47]. A self-assembly study using analytical ultracentrifugation in phosphate buffer has shown that *Mt*PRS in the absence of ligands (R5P, ATP, and ADP) reaches a dynamic equilibrium between trimeric and hexameric aggregation states [26]. These authors also showed that *Mt*PRS dynamic equilibrium shifted toward the hexameric state with concomitant reduction in trimeric species in the presence of ADP [26]. This shift could be related to human PRS isoform 1 [10] and *B. subtilis* [19] ADP binding site identification on the interface of three subunits in the hexamer, a quaternary structure that might be

stabilized by the presence of ADP in solution. On the other hand, analytical gel filtration results suggested that *Mt*PRS eluted as a single symmetrical peak consistent with the hexameric state in phosphate buffer [27]. The data here presented on glutaraldehyde cross-linking (**Figure 4**) and elution of a single peak from Superdex 200 size exclusion column (protein purification protocol) suggest that *Mt*PRS exists as a hexamer in Tris-HCl buffer and absence of ligands. Further efforts are thus needed to ascertain whether or not *Mt*PRS exists in a dynamic equilibrium or as a single oligomeric state under the experimental conditions here described.

PRS enzyme activity is often assessed by radiochemical assays with either [^{14}C]-R5P [26] or [γ-^{32}P]-ATP detection [10, 22, 46, 48], by enzyme coupling with myokinase, pyruvate kinase and lactate dehydrogenase [49], or by a recently developed HPLC-based method that follows AMP formation [27]. Here we present, to the best of our knowledge, a novel coupled continuous spectrophotometric assay that measures the decrease in orotate catalyzed by *Mt*OPRT in the presence of PRPP formed in solution by *Mt*PRS enzyme activity. *Mt*PRS-catalyzed PRPP formation could be measured in the presence of R5P and Mg^{2+}-ATP and absence of P_i (**Figure 5A**), and no enzyme activity could be detected in the presence of 10-50 mM concentrations of inorganic phosphate. Interestingly, it has been reported that *Mt*PRS requires P_i for activity [26, 27]. The reason for this discrepancy is not apparent at the moment. However, it may be speculated that measurements of *Mt*PRS enzyme activity here presented were carried out in the complete absence of P_i since the enzyme was stored in Tris HCl 50 mM pH 7.5 and activity measurements assessed in Tris-HCl 50 mM $MgCl_2$ 20 mM pH 8.0, OA 100 μM, *Mt*OPRT 1.3 μM, and varied concentrations of ATP and R5P. No dependence of *Mt*PRS activity upon varying Mg^{2+} concentrations could be assessed as this cation is

also essential for activity of *Mt*OPRT coupled enzyme [A. Breda, L. A. Rosado, D. M. Lorenzini, L. A. Basso, and D. S. Santos, submitted for publication]. We have thus fixed the Mg^{2+} concentration at 20 mM based on both the optimum concentration for activity of *Mt*OPRT coupled enzyme (larger concentration values are inhibitory) and saturating Mg^{2+} concentration for *Mt*PRS [27]. It has been shown that *Mt*PRS requires free Mg^{2+} as an activator and as Mg^{2+}-ATP co-substrate, and free Mg^{2+} behaves as an allosteric effector of the K-type enzyme model for cooperativity [27]. Substrate specificity measurements showed that *Mt*PRS can accept Mg^{2+}-ATP, Mg^{2+}-GTP, Mg^{2+}-CTP, and Mg^{2+}-UTP as diphosphoryl group donors (**Figure 5B**), thereby showing broad substrate specificity. Interestingly, increasing Mg^{2+}-UTP concentrations seems to reduce *Mt*PRS enzyme activity (**Figure 5B**). It is thus tempting to speculate that UTP produced by uridylate kinase (*pyrH*) and nucleoside diphosphate kinase (*ndkA*) conversion of, respectively, UMP$\rightarrow$UDP$\rightarrow$UTP can indicate that there is no need to synthesize PRPP, a substrate of orotate phosphoribosyl transferase enzyme of the *de novo* pyrimidine nucleotide synthesis.

The purine nucleoside diphosphates (ADP and GDP) inhibited *Mt*PRS enzyme activity with IC_{50} values of, respectively, 802 μM and 86 μM (**Figure 6**). ADP has been shown to be a non-competitive inhibitor of *Mt*PRS with an overall inhibition constant values ranging from 320 μM to 522 μM [26]. On the other hand, it has been reported an IC_{50} value of 0.4 mM for ADP and an IC_{50} larger than 5 mM for GDP inhibition of *Mt*PRS activity in the presence of P_i [27]. These authors also showed that half-maximal inhibition increased with increasing P_i concentration, thereby implying the presence of a regulatory site to which both inhibitory ADP and P_i could bind to [27]. In addition, the sigmoidal curve for ADP inhibition of *Mt*PRS has been

shown to affect the maximum velocity only, without affecting the value of *K'* and the degree of cooperativity [27].

Hyperbolic binding isotherms determined from fluorescence spectroscopy titration indicate that substrates R5P (**Figure 7A**, K_D = 61 μM), and ATP (**Figure 8A**, K_D = 18 μM), and GTP (**Figure 8B**, K_D = 21 μM), an alternative diphosphoryl donor, bind to free *Mt*PRS in a hyperbolic manner. The K_D value for ATP is similar to one previously reported [26]. However, the data here reported for R5P were best fitted to a hyperbolic equation (**Eq. 3**), in disagreement with sigmoidal binary complex formation reported elsewhere with *K'* value of 61 μM [26]. Dissociation constant values for ATP and GTP are similar, an indicative that there might be no substrate preference between these purine 5'-triphosphate nucleotides. Although we have shown that CTP and UTP can act as diphosphoryl group donors, no binary complex formation could be detected by fluorescence spectroscopy in the absence of R5P. These results suggest an alternative order of substrate addition for pyrimidine 5'-triphosphate nucleotides. No PRPP binding to free enzyme could be detected. On the other hand, AMP product showed positive homotropic cooperativity upon binding to free *Mt*PRS, with *K'* value of 109 μM and Hill coefficient value of 3.2 (**Figure 7B**). Data on steady-state kinetics and equilibrium binary complex formation suggest that the enzyme mechanism of *Mt*PRS for purine (ATP and GTP) diphosphoryl donors follows a random-order of substrate addition and ordered product dissociation, in which PRPP is the first product to be released followed by purine nucleoside monophosphate products (AMP or GMP) to yield free enzyme for the next round of catalysis (**Figure 9A**). On the other hand, the enzyme mechanism for pyrimidine (UTP or CTP) diphosphate donors follows an ordered mechanism of substrate addition in which R5P binds to free enzyme followed by the diphosphate donors, and

PRPP release is followed by pyrimidine nucleoside monophosphate products (UMP or CMP) to yield free *Mt*PRS (**Figure 9B**).

*Mt*PRS has approximately 41% identity to the three human PRS isoforms, as well as to *A. thaliana* and spinach Class I enzymes (isoforms 1 and 2). The degree of primary sequence conservation drops to 18-23% when the *M. tuberculosis* sequence is compared to Class II PRS enzymes from the latter two organisms (isoforms 3 and 4). As previously demonstrated [10, 22, 26], the amino acids involved in substrate binding are the most conserved regions: *Mt*PRS Tyr88-Ser104 and Asp166-Arg169 for ATP binding, and *Mt*PRS Asp219-Thr227 for R5P binding. All amino acids involved in ADP allosteric site, according to *B. subtilis* quaternary structure [19], are conserved in *Mt*PRS (Ser43, Arg45, Ser77, Ala78, Lys96, His97, Arg98, Gly99, Arg100, Gln131, Asp139, His140, Ser306 and Phe311), in agreement with the inhibition data presented in **Figure 6A** and with previous reports showing that ADP is an allosteric inhibitor of *Mt*PRS [26, 27]. Despite low amino acid conservation, secondary structure prediction showed that homotrimeric spinach PRS isozyme 4 (a Class II enzyme) and hexameric *B. subtilis* PRS (a Class I enzyme) have a similar folding pattern [20], which corroborates what corroborate the results presented here for *Mt*PRS quaternary structure assembly (**Figure 4**). No Class II PRS structure has been solved so far, thus any inferences about amino acids substitution that might account for the broader substrate specificity are, based on available structural data, speculative. PRS nucleotide binding pocket is located in a wide cleft, and the secondary structure elements might undergo conformational rearrangements upon ligand binding to accommodate both purine and pyrimidine bases, as well as properly positioning of amino acids side chains to specifically hydrogen bond each diphosphoryl group donor.

The broad specificity for diphosphoryl group donors and detection of enzyme activity in the absence of P_i would suggest that *Mt*PRS belongs to Class II PRS proteins. On the other hand, the hexameric quaternary structure (**Figure 4**) would indicate that it belongs to Class I PRS enzymes. In addition, allosteric inhibition by ADP [26, 27] would place *Mt*PRS in Class I PRSs. Accordingly, it has previously been suggested that *Mt*PRS belongs to Class I [27]. Further data are thus needed to classify *Mt*PRS as belonging to a particular family of PRS proteins.

It should be pointed out that the results here presented extend previous studies on *Mt*PRS [26, 27]. To the best of our knowledge, the results here presented are the first experimental evidence for a bacterial PRS enzyme that can use both pyrimidine and purine nucleosides triphosphates as diphosphoryl group donors since broad substrate specificity had been described for plants only. In addition, this is the first report on *Mt*PRS enzyme mechanism for purine and pyrimidine diphosphate donors. Current efforts are towards experimental structure determination of *Mt*PRS to provide a solid foundation for the rational design of, hopefully, specific inhibitors of this enzyme without affecting to a great extent PRS from the host.

Acknowledgments

Conceived and designed the experiments: AB, LAB, and DSS. Performed the experiments: CBB, AB, LKBM, CVB, and LAR. Analyzed the data: AB, CVB, LKBM, and LAR. Contributed reagents/materials/analysis tools: LAB and DSS. Wrote the paper: AB, LAB, and DSS.

References

1. World Health Organization (2010) Global Tuberculosis Control 2010. Geneva: WHO Press.

2. World Health Organization (2010) The Global Plan to Stop TB 2011-2015: Transforming the fight towards elimination of tuberculosis. Available: http://www.stoptb.org. Accessed 2011 April 04

3. Ma Z, Lienhardt C, McIlleron H, Nunn AJ, Wang X (2010) Global tuberculosis drug development pipeline: the need and the reality. Lancet 375: 2100-2109.

4. World Health Organization (2009) A ministerial meeting of high M/XDR-tb burden countries. Available: http://www.who.int/tb/challenges. Accessed 2011 April 16

5. Aziz MA, Wright A, Laszlo A, Muynck AD, Portaels F, et al. (2006) Epidemiology of antituberculosis drug resistance (the global project on anti-tuberculosis drug resistance surveillance): an updated analysis. Lancet 368: 2142-2154.

6. Svenson S, Källenius G, Pawlowski A, Hamasur B (2010) Towards new tuberculosis vaccines. Human Vaccines 6: 309-317.

7. Velayati AA, Masjedi MR, Farnia P, Tabarsi P, Ghanavi J, et al. (2009) Emergence of new forms of totally drug-resistant tuberculosis bacilli super extensively drug-resistant tuberculosis or totally drug-resistant strains in Iran. Chest 136: 420-425.

8. Ducati RG, Basso LA, Santos DS (2007) Mycobacterial shikimate pathway enzymes as targets for drug design. Curr Drug Targets 8: 423-435.

9. Khorana HG, Fernandes JF, Kornberg A (1958) Pyrophosphorylation of ribose 5-phosphate in the enzymatic synthesis of 5-phosphorylribose 1-pyrophosphate. J Biol Chem 230: 941–948.

10. Li S, Lu Y, Peng B, Ding J (2007) Crystal structure of human phosphoribosylpyrophosphate synthetase 1 reveals a novel allosteric site. Biochem J 401: 39-47.

11. Hove-Jensen B (1988) Mutation in the phosphoribosylpyrophosphate synthetase gene (prs) that results in simultaneous requirements for purine and pyrimidine nucleosides, nicotinamide nucleotide, histidine, and tryptophan in *Escherichia coli*. J Bacteriol 170: 1148–1152.

12. Ames BN, Martin RG, Garry BJ (1961) The first step of histidine biosynthesis. J Biol Chem 236: 2019-2026.

13. Zoref E, De Vries A, Sperling O (1975) Mutant feedback-resistant phosphoribosylpyrophosphate synthetase associated with purine overproduction and gout. J Clin Invest 56: 1093-1099.

14. Scherman MS, Kalbe-Bournonville L, Bush D, Xin Y, Deng L, et al. (1996) Polyprenylphosphate-pentoses in mycobacteria are synthesized from 5-phosphoribose pyrophosphate. J Biol Chem 271: 29652-29658.

15. Wolucka BA (2008) Biosynthesis of D-arabinose in mycobateria - A novel bacterial pathway with implication for antimycobaterial therapy. FEBS J 275: 2691-2711.

16. Hove-Jensen B, Harlow KW, King CJ, Switzer RL (1986) Phosphoribosylpyrophosphate synthetase of *Escherichia coli*. Properties of the purified enzyme and primary structure of the prs gene. J Biol Chem 261: 6765-6771.

17. Switzer L (1969) Regulation and mechanism of phosphoribosylpyrophosphate synthetase I: Purification and properties of the enzyme from *Salmonella typhimurium.* J Biol Chem 244: 2854-2863.

18. Tatibana M, Kita K, Taira M, Ishijima S, Sonoda T, et al. (1995) Mammalian phosphoribosylpyrophosphate synthetase. Adv Enzyme Regul 35: 229-249.

19. Eriksen TA, Kadziola A, Bentsen AK, Harlow KW, Larsen S (2000) Structural basis for the function of *Bacillus subtilis* phosphoribosyl-pyrophosphate synthetase. Nat Struct Biol 7: 303–308.

20. Krath BN, Hove-Jensen B (2001) Implications of secondary structure prediction and amino acid sequence comparison of class I and class II phosphoribosyl diphosphate synthases on catalysis, regulation, and quaternary structure. Protein Sci 10: 2317-2324.

21. Sinha SC, Smith JL (2001) The PRT protein family. Curr Opin Struct Biol 11: 733-739.

22. Kadziola A, Jepsen CH, Johansson E, McGuire J, Larsen S, et al. (2005) Novel class III phosphoribosyl diphosphate synthase: structure and properties of the tetrameric, phosphate-activated, non-allosterically inhibited enzyme from *Methanocaldococcus jannaschii*. J Mol Biol 354: 815-828.

23. Krath BN, Hove-Jensen B (2001) Class II recombinant phosphoribosyl diphosphate synthase from spinach. J Biol Chem 276: 17851-17856.

24. Krath BN, Eriksen TA, Poulsen TS, Hove-Jensen B (1999) Cloning and sequencing od cDNAs specifying a novel class of phosphoribosyl diphosphate synthase in Arabdopsis thaliana. Biochim Biophys Acta 1430: 403-408.

25. Sassetti CM, Boyd DH, Rubin EJ (2003) Genes required for mycobacterial growth defined by high density mutagenesis. Mol Microbiol 48: 77-84.

26. Alderwick LJ, Lloyd GS, Lloyd AJ, Lovering AL, Eggeling L, et al. (2011) Biochemical characterization of the *Mycobacterium tuberculosis* phosphoribosyl-1-pyrophosphate synthetase. Glycobiology 21: 410-425.

27. Lucarelli AP, Buroni S, Pasca MR, Rizzi M, et al. (2010) *Mycobacterium tuberculosis* phosphoribosylpyrophosphate synthase: Biochemical features of a crucial enzyme for mycobacterial cell wall biosynthesis. PloS ONE 5(11): e315494.

28. Boshoff HIM, Barry CE (2005) Tuberculosis - metabolism and respiration in the absence of growth. Nat Rev Micro 3: 70-80.

29. Laemmli UK (1970) Cleavage of structural proteins during the assembly of the head of bacteriophage T4. Nature 227: 680-685.

30. Bradford MM, Mcrorie RA, Williams WL (1976) A rapid and sensitive method for the quantitation of microgram quantities of protein utilizing the principle of protein-dye binding. Anal Biochem 72: 248-254.

31. Klammer AA, MacCoss MJ (2006) Effects of modified digestion schemes on the identification of proteins from complex mixtures. J Proteome Res 5: 695-700.

32. Moritz RL (2007) Configuration, column construction, and column packing for a capillary liquid chromatography system. CSH Protocols. doi: 10.1101/pdb.prot4578.

33. Zhang Z, Marshall AG (1998) A universal algorithm for fast and automated charge state deconvolution of electrospray mass-to-charge ratio spectra. J Am Chem Soc Mass Spectrom 9: 225-233.

34. Fadouloglou VE, Kokkinidis M, Glykos NM (2008) Determination of protein oligomerization state: two approaches based on glutaraldehyde crosslinking. Anal Biochem 373: 404–406.

35. Krungkrai SR, Del Fraino BJ, Smiley JA, Prapunwattana P, Mitamura T, et al. (2005) A novel enzyme complex of orotate phosphoribosyltransferase and orotidine 5'-monophosphate decarboxylase in human malaria parasite Plasmodium falciparum: physical association, kinetics, and inhibition characterization. Biochemestry 44: 1643-1652.

36. Copeland RA (2005) Evaluation of enzyme inhibitors in drug discovery. John Wiley and Sons, Inc., New Jersey.

37. Tamura K, Peterson D, Peterson N, Stecher G, Nei M, et al. (2011) MEGA5: Molecular evolutionary genetics analysis using maximum likelihood, evolutionary distance, and maximum parsimony methods. Mol Biol Evol. In press.

38. Hill AV (1913) The combinations of haemoglobin with oxygen and with carbon monoxide. J Biochem 7: 471-480.

39. Segel IH (1975) Enzymes kinetics – Behavior and analysis of rapid equilibrium and steady-state enzyme systems. John Wiley & Sons, Inc., New York, 360 p.

40. Martinelli LKB, Ducati RG, Rosado LA, Breda A, Selbach BP, et al. (2011) Recombinant *Escherichia coli* GMP reductase: kinetic, catalytic and chemical

mechanisms, and thermodynamics of enzyme–ligand binary complex formation. Mol Biosyst 7: 1289-1305.

41. Kelley KC, Huestis KJ, Austen DA, Sanderson CT, Donoghue MA, et al. (1995) Regulation of *sCD4-183* gene expression from phage-T7-based vectors in *Escherichia coli.* Gene 156: 33-36.

42. Grossman TH, Kawasaki ES, Punreddy SR, Osburne MS (1998) Spontaneous cAMP-dependent derepression of gene expression in stationary phase plays a role in recombinant expression instability. Gene 209: 95-103.

43. Studier FW (2005) Protein production by auto-induction in high density shaking cultures. Protein Expr Purif 41: 207-234.

44. Chant A, Kraemer-Pecore CM, Watkin R, Kneale GG (2005) Attachment of a histidine tag to the minimal zinc finger protein of the *Aspergillus nidulans* gene regulatory protein AreA causes a conformational change at the DNA-binding site. Protein Expr Purif 39: 152-159.

45. Fonda I, Kenig M, Gaberck-Porekar V, Prostovaek P, Menart V (2002) Attachment of histidine tags to recombinant tumor necrosis factor-alpha drastically changes its properties. Sci World J 2: 1312-1325.

46. Arnvig K, Hove-Jensen B, Switzer RL (1990) Purification and properties of phosphoribosyl-diphosphate synthetase from *Bacillus subtilis*. Eur J Biochem 192: 195-200.

47. Schubert KR, Switzer RL (1975) Studies of the quaternary structure and the chemical properties of phosphoribosylpyrophosphate synthetase from *Salmonella typhimurium*. J Biol Chem 250: 7492-7500.

48. Nosal JM, Switzer RL, Becker MA (1993) Overexpression, purification, and characterization of recombinant human 5-phosphoribosyl-1-pyrophosphate synthetase isozymes I and II. J Biol Chem 268: 10168-10175.

49. Braven J, Hardwell TR, Seddon R, Whittaker M (1984) A spectrophotometric assay of phosphoribosyl pyrophosphate synthetase. Ann Clin Biochem 21: 366-371.

Figure Legends

Figure 1. Chemical reaction catalyzed by *Mt*PRS (Rv1017c). This figure also shows the metabolic source of R5P and the biosynthetic pathways in which the reaction product PRPP plays central roles.

Figure 2. *Mt*PRS purification steps. Lane 1: Protein marker – Fermentas (116, 66.2, 45, 35, 25, 18.4 and 14.4 kDa); lane 2: crude extract; lane 3: sample eluted from anion exchange step; lane 4: protein fraction from size exclusion chromatography step showing elution of homogeneous recombinant *Mt*PRS (approximately 35 kDa).

Figure 3. LC-MS/MS deconvoluted spectra, corresponding to average *Mt*PRS molecular mass of 35,345 Da. The spectra also corroborate *Mt*PRS homogeneity after two-step purification protocol, for the absence of contaminants detection.

Figure 4. *Mt*PRS quaternary structure assignment by glutaraldehyde cross-linking experiments. Lane 1: *M. tuberculosis* IMPDH (55 and 219 kDa); lane 2: Page Ruler – Fermentas (200, 150, 120, 100, 85, 70, 60, 50, 40, 30, 25, 20, 15 and 10 kDa); lane 3: *Mt*PRS without incubation – negative control, lane 4: *Mt*PRS 10 min incubation; lane 5: *Mt*PRS 20 min incubation; lane 6: *Mt*PRS 30 min incubation; lane 7: *Mt*PRS 40 min incubation.

Figure 5. *Mt*PRS activity measured under standard assay conditions, using Mg^{2+}-ATP (A), or Mg^{2+}-GTP, Mg^{2+}-CTP, and Mg^{2+}-UTP (B) as diphosphoryl group donors.

Figure 6. Inhibition of *Mt*PRS enzyme activity by ADP (A) and GDP (B). Percentage of fractional *Mt*PRS enzyme activity was plotted against ADP (A) and GDP (B) concentrations, considering 100% enzyme activity in the absence of these nucleoside diphosphates.

Figure 7. Equilibrium binding of R5P (A) and AMP (B) to *Mt*PRS using fluorescence spectroscopy.

Figure 8. Equilibrium binding of ATP (A) and GTP (B) to *Mt*PRS using fluorescence spectroscopy.

Figure 9. Proposed enzyme mechanisms for *Mt*PRS using purines (A) or pyrimidines (B) 5'-trisphosphate nucleotides as diphosphoryl group donors. Random order of addition for ATP or GTP (A) and ordered addition of UTP or CTP (B) substrates, and ordered release of products.

Figure 1
Click here to download high resolution image

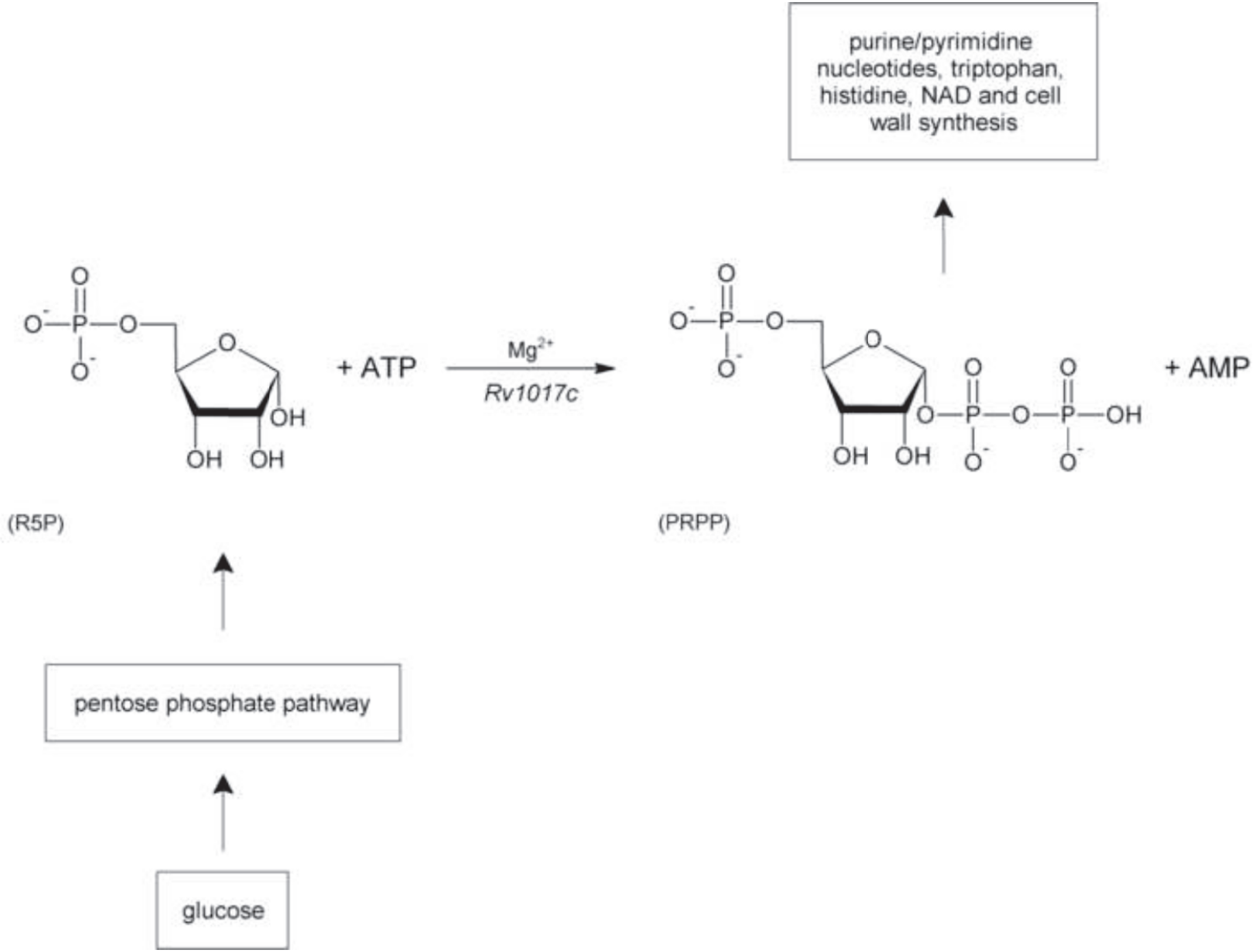

Figure 2
Click here to download high resolution image

Figure 3
Click here to download high resolution image

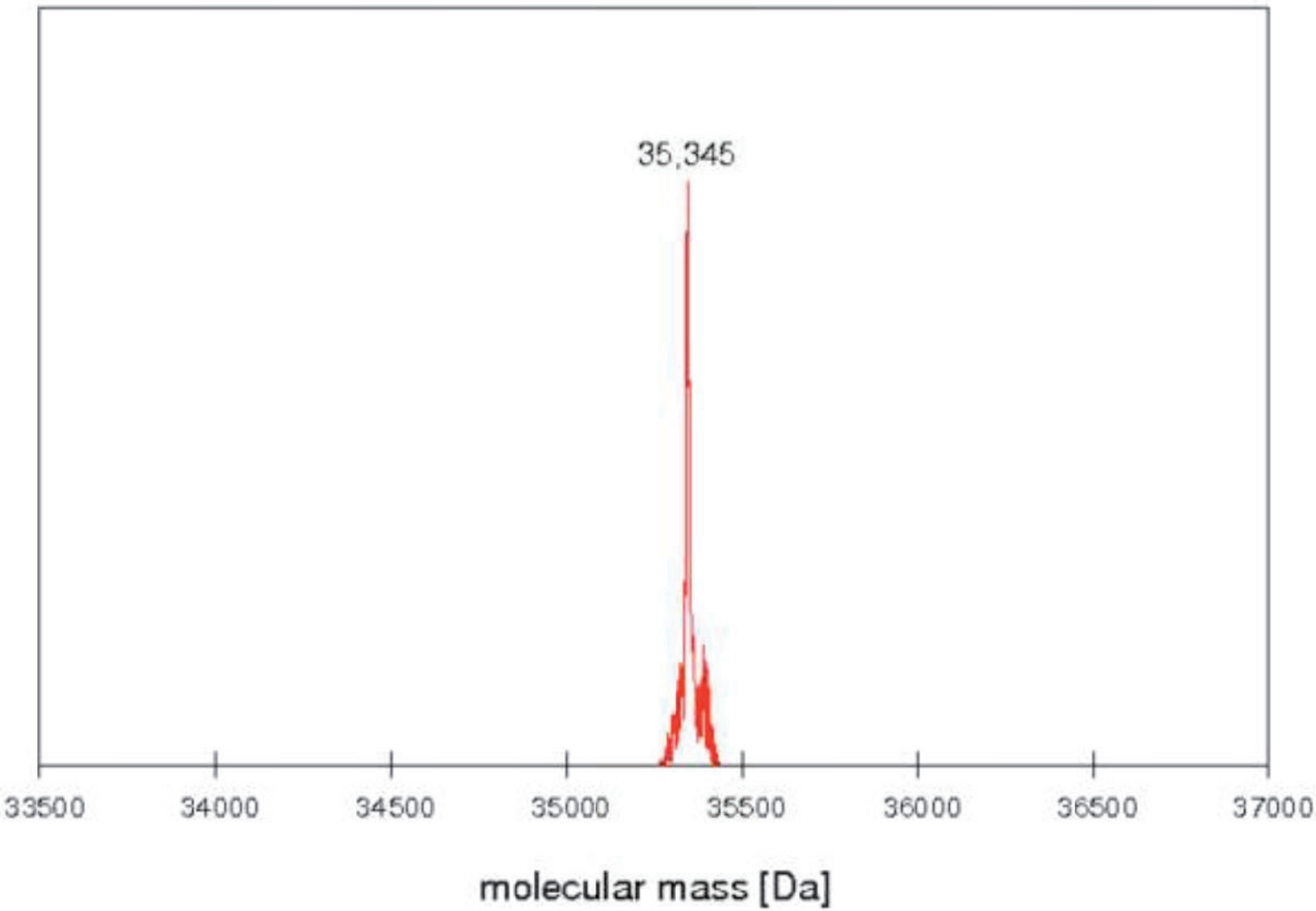

Figure 4
Click here to download high resolution image

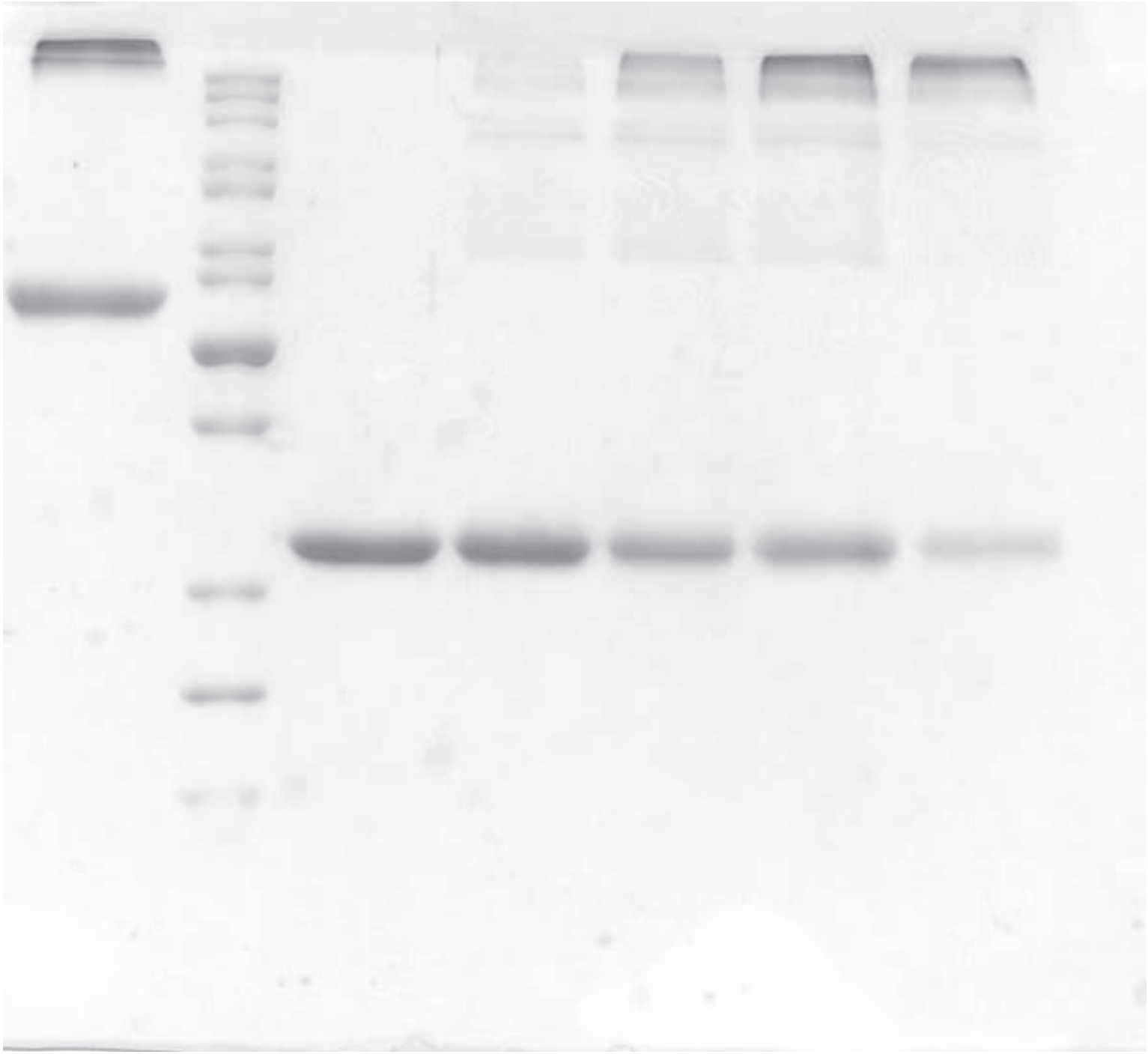

Figure 5
Click here to download high resolution image

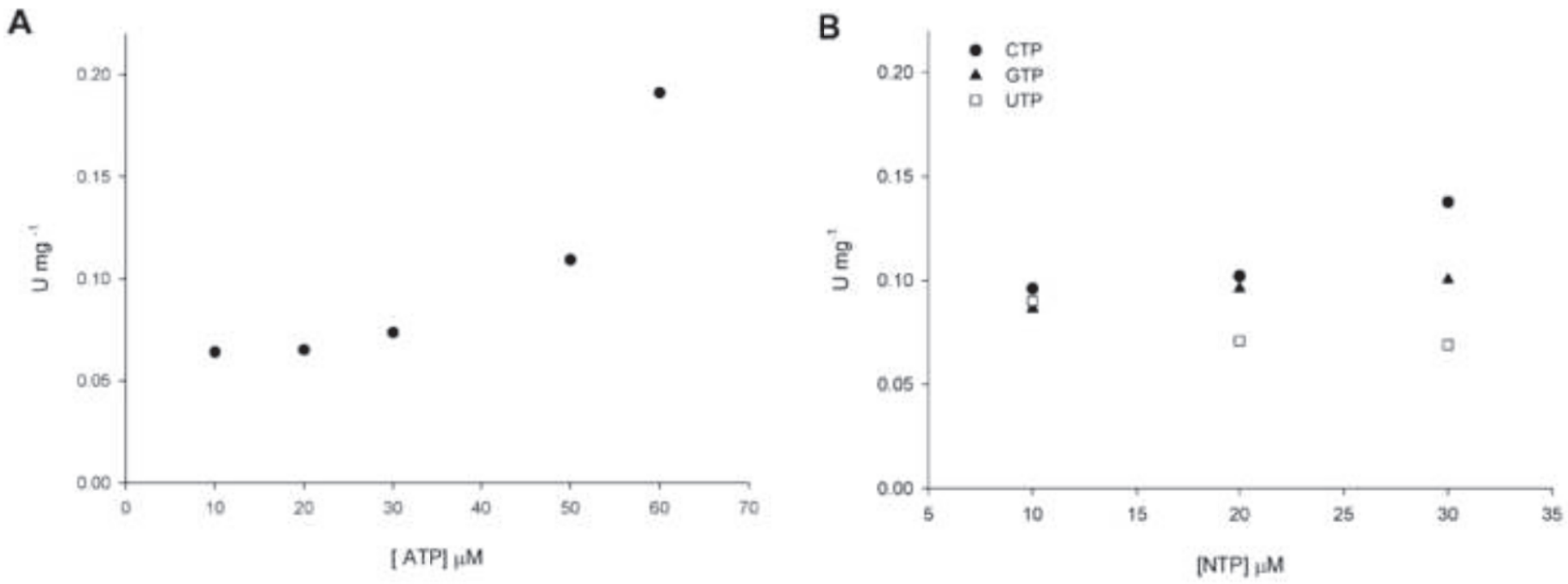

Figure 6
Click here to download high resolution image

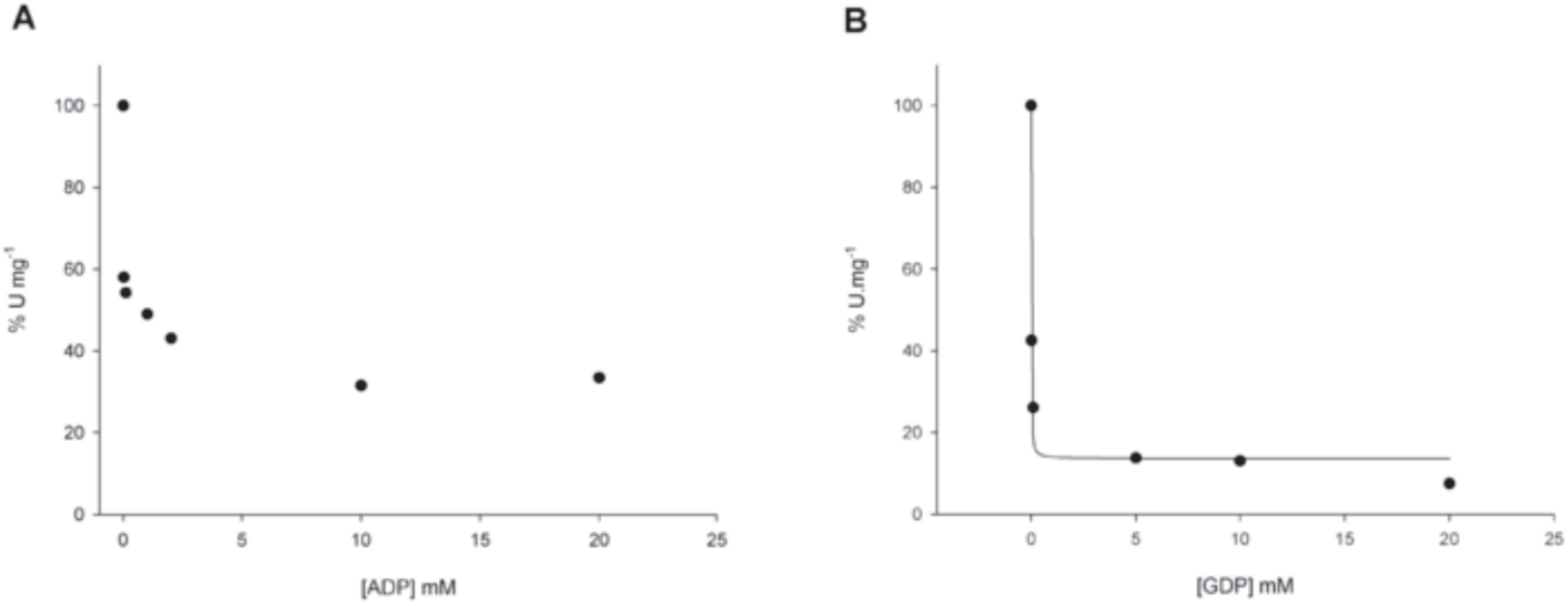

Figure 7
Click here to download high resolution image

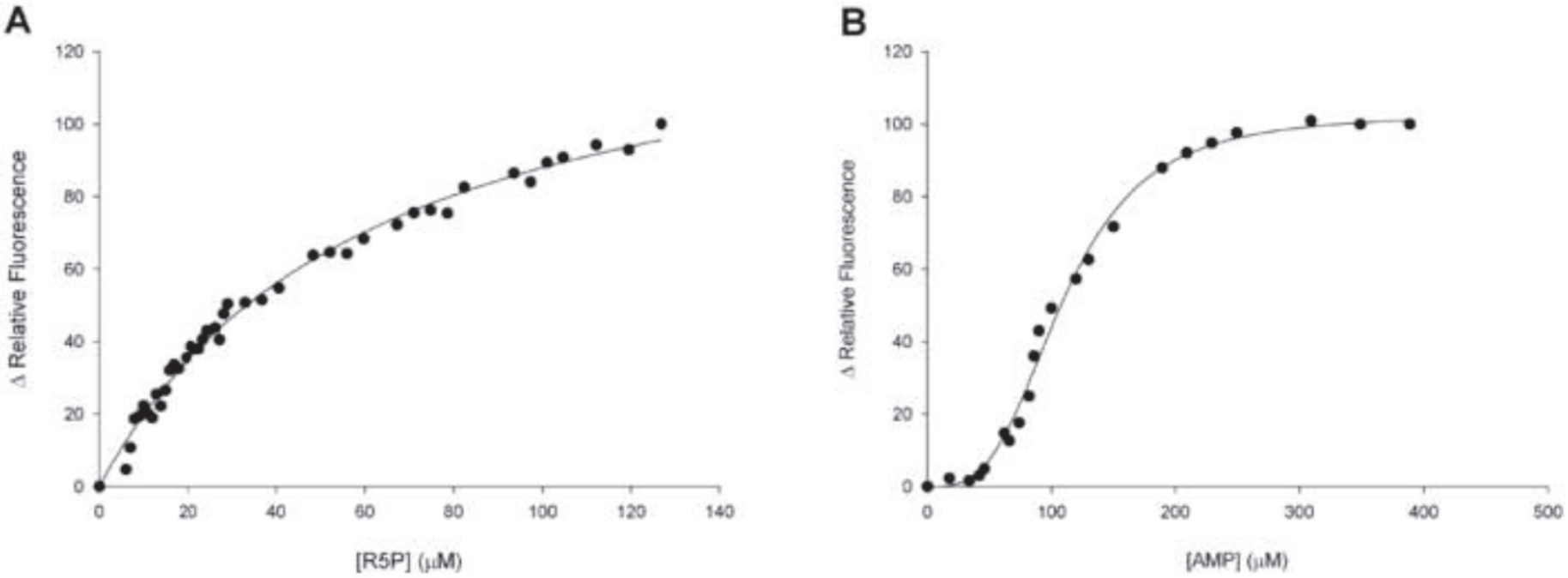

Figure 8
Click here to download high resolution image

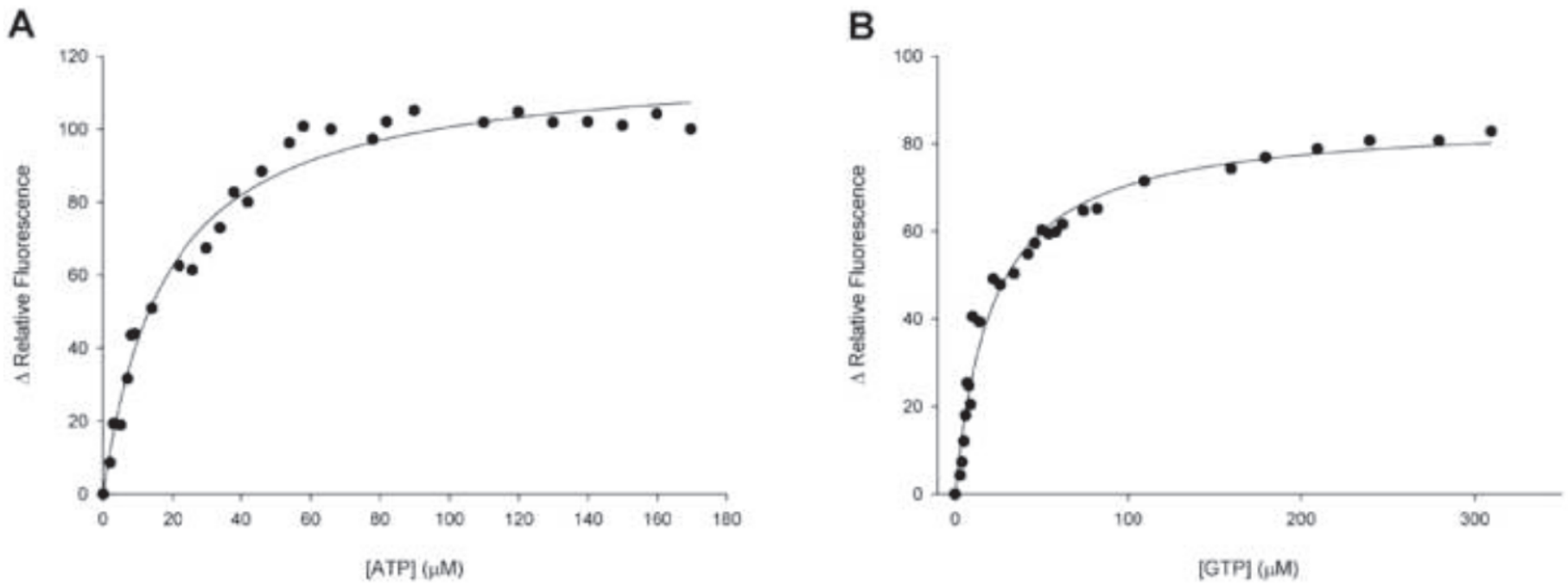

Figure 9
Click here to download high resolution image

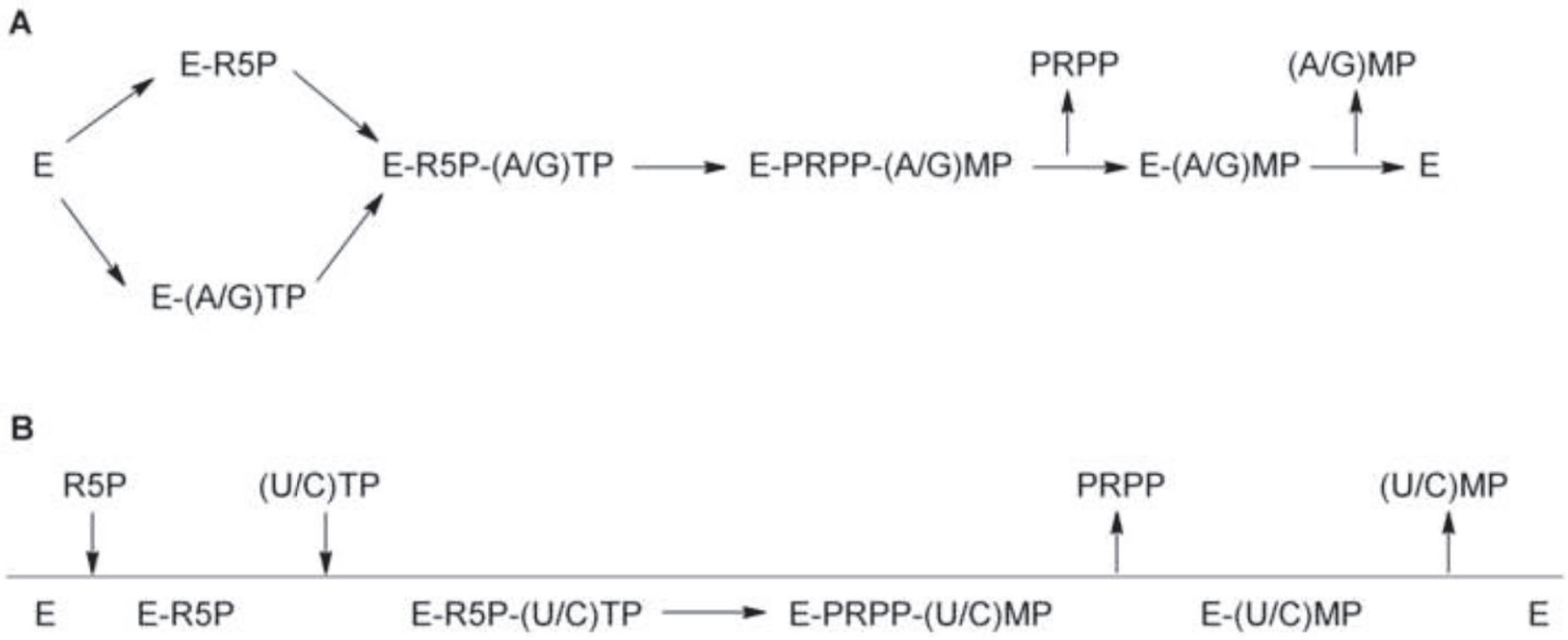

Table 1
Click here to download Table: Table1.doc

Table 1. Purification of *Mt*PRS from 4 g of wet cell paste of *E. coli* BL21(DE3) host cells.

Step	*Total protein (mg)*	*Specific activity (U mg^{-1})*	*Total enzyme activity (U)*	*Yield %*	*Purification fold*
crude extract	283	0.023	6.67	100	1
Q-Sepharose	14.3	0.208	2.92	44	8.8
Superdex 200	2.6	0.237	0.62	9.3	10

4. Considerações finais

A tuberculose tornou-se altamente controlada com o programa DOTS reforçado pelo sucesso da quimioterapia, mas nunca realmente desapareceu. Hoje em dia, a tuberculose ainda representa uma ameaça global, tornando-se causa líder de morte em adultos devido a um único agente infeccioso, o *Mycobacterium tuberculosis*, responsável por cerca de dois milhões de mortes por ano no mundo [16, 6, 5]. Terapias antimicobacteriais existem, porém drogas atualmente disponíveis são parcialmente eficazes devido à natureza impermeável da parede celular micobacterial e a propensão do bacilo em desenvolver resistência [52]. Agentes quimioterápicos mais eficazes e menos tóxicos são necessários para reduzir a duração do tratamento atual, assim como melhorar as possibilidades de tratamento para as cepas MDR-TB, XDR-TB e TDR-TB. Além disso, há a necessidade de um tratamento eficaz para a TB latente, impedindo que a doença se desenvolva para a forma ativa, e também drogas que não interfiram com os anti-retrovirais para que possam ser utilizados em pacientes co-infectados com HIV [22].

O desenho racional de uma droga é normalmente baseado no estudo da bioquímica e a fisiologia básica do organismo, com a caracterização molecular, bioquímica e cinética de alvos moleculares específicos responsáveis pela doença [53].

O gene *prsA*, que codifica a enzima PRS de *M. tuberculosis*, foi amplificado por PCR e clonado em vetor de expressão pET23a(+). A proteína recombinante foi superexpressa em células de *E. coli* BL21(DE3) sem a presença de IPTG.

Diferentes colunas cromatográficas foram testadas a fim de determinar um protocolo eficiente de purificação. A proteína homogênea foi obtida através de dois passos cromatográficos (troca aniônica e gel filtração). O protocolo desenvolvido resulta em uma forma homogênea e também estável da enzima, sem perda significativa de atividade quando armazenada em ultrafreezer (-80ºC), por até 7 meses e adequada para a realização de ensaios posteriores.

A caracterização molecular da enzima através do sequenciamento da sua estrutura primaria e a determinação da sua estrutura quaternária por cross-linking nos mostra que a enzima é um hexâmero em solução.

Os ensaios espectrofométricos de atividade e de inibição pelos produtos da reação, juntamente com os resultados obtidos pelos ensaios de ligação realizadas em espectrofotômetro permitiram à identificação dos substratos doadores de grupamento difosforil (ATP, CTP, GTP, e UTP), a não dependência de P_i para a atividade da enzima de Mtb e a atividade inibitória dos nucleosídeos difosfato ADP e GDP. Os ensaios de ligação dos substratos e produtos no espectrofotômetro de fluorescência permitiram a determinação do mecanismo cinético da reação. Através do ensaio de ligação, vimos que os substratos R5P, ATP e GTP e o produto AMP são capazes de se ligarem à enzima na sua forma livre, indicando um provável mecanismo sequencial aleatório para nucleotídeos de purina, com liberação sequencial ordenada dos produtos; e mecanismo sequencial ordenado para a ligação dos substratos e liberação dos produtos para nucleotídeos de pirimidina.

Recentemente, Alderwick e colaboradores [54], Lucarelli e colaboradores [55] publicaram a caracterização bioquímica de PRS de Mtb, onde mostraram sua essencialidade, caracterização cinética, e ensaios de inibição. Os

resultados do trabalho apresentado nesta dissertação de mestrado, e compilados no artigo cientifico “Wild-type Phosphoribosylpyrophosphate Synthase (PRS) from Mycobacterium tuberculosis: a Bacterial Class II PRS?", apresentado no Item 3, corroboram os dados anteriormente apresentados [54, 55], e incluem ainda resultados não descritos e uma nova técnica de ensaio cinético continuo para a monitoração da atividade de enzimas PRS.

Diferentemente do que foi publicado anteriormente [54, 55], onde ocorre à utilização de cauda de histidina, mostramos que a PRS de Mtb foi purificada apenas em duas etapas, sem utilização de cromatografia de afinidade, descartando assim a necessidade do uso da cauda de histidina para expressão da enzima. Além disso, os ensaios de atividade já utilizados são radioquímicos, por acoplamento com as enzimas miocinase, piruvato quinase e lactato desidrogenase [56], ou por métodos descontínuos em HPLC [55]. A detecção da atividade *Mt*PRS foi realizado através do monitoramento do consumo de orotado, em um ensaio acoplado com a enzima *Mt*OPRT. Esta metodologia nos permitiu verificar que a enzima PRS é capaz de catalisar a conversão de R5P em PRPP não apenas na presença de ATP, mas também utilizando GTP, CTP e UTP como doadores do grupamento difosforil, atividade que até então não havia sido descrita. Foi possível detectar ainda a não dependência de P_i para a atividade catalítica da PRS de Mtb. Estas características são indicativas de que a enzima PRS de Mtb pode ser classificada como uma provável PRS classe II, classe que até então só havia sido identificada em plantas.

Este trabalho resultou na caracterização da enzima PRS de Mtb como potencial alvo para o desenvolvimento de inibidores. Embora a enzima de Mtb possua 41% de identidade com as isoforma de PRS humanas, aqui mostramos

que há uma diferença significante entre elas, pois a PRS humana utiliza somente ATP como substrato doador de grupamento difosforil, e a PRS de Mtb utiliza também GTP, CTP e UTP na reação. Desta maneira, inibidores seletivos da enzima PRS que sejam baseados nos nucleotídeos GTP, CTP e UTP, e não em ATP, potencialmente não terão ação inibitória sobre a forma humana. Futuros estudos bioquímicos e estruturais serão realizados, a fim de identificar os resíduos de aminoácidos responsáveis pela diferente afinidade de substrato apresentada pela enzima de Mtb e para avaliar possíveis moléculas inibidoras que possam ser testadas no tratamento da TB.

Referências Bibliográficas

[1] Saunders BM, Britton WJ. Life and death in the granuloma: immunopathology of tuberculosis. Immunol cell biol. 2007; 85:103-111.

[2] Palomino JC, Leão SC, Ritacco V. Tuberculosis 2007- From Basic Science to Patient Care. First edition. Disponível em: www.tuberculosistextbook.com. Acesso em: maio de 2011.

[3] Core Curriculum on Tuberculosis: What the Clinician Should Know, 4th edition (2000). Publicado pela Division of Tuberculosis Elimination dos EUA. Disponível em: http://www.cdc.gov/tb/pubs/corecurr. Acesso em: maio de 2011.

[4] Bloom BR, Murray CJL. Tuberculosis: Commentary on a Reemergent Killer. Science. 1992; 257:1055-1064.

[5] WHO: Report WHO/HTM/TB/2008.393, (2008). Página da organização Mundial da Saúde. Disponível em: http://www.who.int/tb/publications/global_report/2008/en/index.html. Acesso em: maio de 2011.

[6] World Health Organization (2010) Global Tuberculosis Control 2010. Geneva : WHO Press.

[7] Disponível em: portal da saúde http://portal.saude.gov.br/portal/saude/profissional/visualizar_texto.cfm?idtxt=31115. Acesso em junho de 2010.

[8] Centers for Disease Control and Prevention (CDC). TB General information, 2008. Disponível em: http://www.cdc.gov/tb/pubs/TBfactsheets.htm. Acesso em: maio de 2011.

[9] Glickman MS, Jacob WR. Microbial pathogenesis of Mycobacterium tuberculosis: dawn of a discipline. Cell. 2001; 104:447-485.

[10] Cole E, Cook C. Characterization of infectious aerosols in health care facilities: an aid to effective engineering controls and preventive strategies. Am J Infect Control.1998;26: 453-464.

[11] Nicas M, Nazaroff WW, Hubbard A. Toward understanding the risk of secondary airborne infection: emission of respirable pathogens. J Occup Environ Hyg. 2005; 2(3):143–154.

[12] Pereira SM, Dantas OMS, Ximenes R, Barreto ML. BCG vaccine against tuberculosis: its protective effect and vaccination policies. Rev. Saúde Pública 2007; 41(1):59-66.

[13] World Health Organization. Treatment of tuberculosis: guidelines for national programmes. WHO, Geneva, 2003.

[14] Ramaswamy S, Musser JM. Molecular genetics basis of antimicrobial agent resistance in Mycobacterium tuberculosis: 1998 update. Tuber Lung Dis. 1998; 79:3-29.

[15] Yew WW, Leung CC. Management of multidrug-resistant tuberculosis: Update 2007. Respirology. 2008; 13:21-46.

[16] Ducati RG, Ruffino-Neto A, Basso LA, Santos DS. The resumption of consumption – A review on tuberculosis. Mem Inst Oswaldo Cruz. 2006; 101:697-714.

[17] Zager EM, McNerney R. Multidrug-resistant tuberculosis. BMC Infect Diseases. 2008; 8:10.

[18] Basso LA, Blanchard JS. Resistance to antitubercular drugs. Adv Exp Med Biol. 1998; 456:115-144.

[19] Hargreaves S. WHO report highlights alarming rise of resistant tuberculosis. Lancet. 2008; 8:220.

[20] Velayati AA, Masjedi MR, Farnia P, Tabarsi P, Ghanavi J, ZiaZarifi AH, Hoffner SE. Emergence of New Forms of Totally Drug-Resistant Tuberculosis Bacilli. CHEST. 2009; 136:420-425.

[21] World Health Organization. Global tuberculosis control: surveillance, planning, financing. WHO Report 2006./WHO/HTM/TB/2006.35. Disponível em: http://www.who.int/tb/publications/global_report/2007/pdf/full.pdf. Acesso em: maio de 2011.

[22] Ginsberg AM, Spigelman M. Challenges in tuberculosis drug research and development. Nature Med. 2007; 13:290-294.

[23] Cole ST, Brosch R, Parkhill J, Garnier T, Churcher C, Harris D, et al. Deciphering the biology of Mycobacterium tuberculosis from the complete genome sequence. Nature. 1998; 393:537-544.

[24] Campos L. Entender a Bioquímica. 2ª ed. Editora Escolar, Portugal, 1999.

[25] Tozzi MG, Camici M, Mascia L, Sgarrella F, Ipata PL. Pentose phosphates in nucleoside interconversion and catabolism. FEBS J. 2006; 273:1089-1101.

[26] Smith CS, Marks AD, Lieberman M. Bioquímica médica Básica de Marks. 2ª edição. Editora Artemed, Brasil, 2007.

[27] Voet D, Voet JG. Bioquímica. 3ª ed. Editora Artmed, Brasil, 2006.

[28] Hager SE, Jones ME. A Glutamine-dependent Enzyme for the Synthesis of Carbamyl Phosphate for Pyrimidine Biosynthesis in Fetal Rat Liver. J. Biol. Chem. 1967; 242:5674-5680.

[29] Hoffmeyer J, Neuhard J. Metabolismo of Exogenous Purine Bases and Nucleosides by Salmonella Typhimurium. J. Bacteriol. 1971; 106:14-24.

[30] Bhagavan NV. Medical biochemistry. 4ª edição. Editora Academic Press, Canadá, 2002.

[31] Switzer RL, Sogin DC. Regulation and Mechanism of Phosphoribosylpyrophosphate Synthetase: V. Inibition by end products and regulation by adenosine diphosphate. J. Biol. Chem. 1973; 248:1063-1073.

[32] Disponível em: http://genolist.pasteur.fr/TubercuList/. Acesso em: junho de 2011.

[33] Schubert KR, Switzer RL, Shelton E. Studies of the quatemary structure & the chemical properties of phosphoribosyl pyrophosphate synthetase from Salmonella typhimurium. J. Biol. Chem. 1975; 250:7492-7500.

[34] Arnvig K, Hove-Jensen B, Switzer RL. Purification and properties of phosphoribosyl-diphosphate synthetase from Bacillus subtilis. Eur. J. Biochem. 1990; 192:195-200.

[35] Carter AT, Narbad A, Pearson BM, Beck KF, Baum B, Logghe M, Contreras R, Schweizer M. Phosphoribosyl pyrophosphate synthetase (PRS): a new gene family in Saccharomyces cerevisiae. Yeast. 1994; 10:1031-1044.

[36] Krath BN, Hove-Jensen B. Organellar and Cytosolic Localization of Four Phosphoribosyl Diphosphate Synthase Isozymes in Spinach. Plant Physiol. 1999; 119:497-505.

[37] Li S, Lu Y, Peng B, Ding J. Crystal structure of human phosphoribosylpyrophosphate synthetase 1 reveals a novel allosteric site. Biochem. J. 2007; 401:39-47.

[38] Wenying T, Xiaowu L, Zhiqiang Z, Shuilong T, Xu L, Xiao Z, Maikun T, Liwen N. Expression, purification, crystallization and preliminary X-ray diffraction analysis of human phosphoribosyl pyrophosphate synthetase 1 (PRS1). Acta Cryst. 2006; 62:432–434.

[39] Hove-Jensen B, Harlow KW, King CJ, Switzer RL. Phosphoribosylpyrophosphate synthetase of *Escherichia coli*. Properties of the purified enzyme and primary structure of the prs gene. J Biol Chem 1986; 261: 6765-6771.

[40] Switzer L. Regulation and mechanism of phosphoribosylpyrophosphate synthetase I: Purification and properties of the enzyme from *Salmonella typhimurium.* J Biol Chem 1969; 244: 2854-2863.

[41] Tatibana M, Kita K, Taira M, Ishijima S, Sonoda T, et al. Mammalian phosphoribosylpyrophosphate synthetase. Adv Enzyme Regul 1995; 35: 229-249.

[42] Eriksen TA, Kadziola A, Bentsen AK, Harlow KW, Larsen S. Structural basis for the function of *Bacillus subtilis* phosphoribosyl-pyrophosphate synthetase. Nat Struct Biol 2000; 7: 303–308.

[43] Zoref E, De Vries A, Sperling O. Mutant feedback-resistant phosphoribosylpyrophosphate synthetase associated with purine overproduction and gout. J Clin Invest 1975; 56:1093-1099.

[44] Krath BN, Hoje-Jensen B. Implications of secondary structure prediction and amino acid sequence comparison of class I and class II phosphoribosyl diphosphate synthases on catalysis, regulation, and quaternary structure. Protein Sci 2001; 10:2317-2324.

[45] Sinha SC, Smith JL. The PRT protein family. Curr Opin Struct Biol 2001; 11:733-739.

[46] Kadziola A, Jepsen CH, Johansson E, McGuire J, Larsen S, et al. Novel class III phosphoribosyl diphosphate synthase: structure and properties of the tetrameric, phosphate-activated, non-allosterically inhibited enzyme from *Methanocaldococcus jannaschii*. J Mol Biol 2005; 354: 815-828.

[47] Krath BN, Hove-Jensen B. Class II recombinant phosphoribosyl diphosphate synthase from spinach. J Biol Chem 2001; 276: 17851-17856.

[48] Krath BN, Eriksen TA, Poulsen TS, Hove-Jensen B. Cloning and sequencing od cDNAs specifying a novel class of phosphoribosyl diphosphate synthase in Arabdopsis thaliana. Biochim Biophys Acta 1999; 1430: 403-408.

[49] Thompson JD, Higgins DG, Gibson TJ. CLUSTAL W: improving the sensitivity of progressive multiple sequence alignment through sequence weighting, position-specific gap penalties and weight matrix choice. Nucleic Acids Res. 1994; 22(22):4673-4680.

[50] Nelson DL, Cox MM. Lehninger - Principles of Biochemistry. 4ª ed. W.H. Freeman and Company, USA, 2005.

[51] Radwanski ER, Last RL. Tryptophan biosynthesis and metabolism: biochemical and molecular genetics. Plant Cell 1995;7(7):921-934.

[52] Pieters J. Mycobacterium tuberculosis and the macrophage: maintaining a balance. Cell Host Microbe. 2008, 3(6):399-407.

[53] Parker WB, Long MC. Purine metabolism in Mycobacterium tuberculosis as a target for drug development. Current pharmaceutical design. 2007;13:599-608.

[54] Alderwick LJ, Lloyd GS, Lloyd AJ, Lovering AL, Eggeling L, et al. Biochemical characterization of the Mycobacterium tuberculosis phosphoribosyl-1-pyrophosphate synthatase. Glycobiology 2011; 21: 410-425.

[55] Lucarelli AP, Buroni S, Pasca MR, Rizzi M, et al. Mycobacterium tuberculosis phosphoribosylpyrophosphate synthase: Biochemical features of a crucial enzyme for mycobacterial cell wall biosynthesis. PloS ONE 2010; 5(11): e315494.

[56] Braven J, Hardwell TR, Seddon R, Whittaker M. A spectrophotometric assay of phosphoribosyl pyrophosphate synthetase. Ann Clin Biochem 1984; 21: 366-371.

ANEXO

Carta de submissão do artigo Wild-type Phosphoribosylpyrophosphate Synthase (PRS) from Mycobacterium tuberculosis: a Bacterial Class II PRS?". à revista PLoS ONE.

From: em.pone.0.257783.3c996a67@editorialmanager.com on behalf of PLoS ONE

Sent: Fri 9/2/2011 2:16 PM

To: Luiz Augusto Basso

Subject: Submission Confirmation for Wild-type Phosphoribosylpyrophosphate Synthase (PRS) from Mycobacterium tuberculosis: a Bacterial Class II PRS?

Dear Dr. Basso,

Your submission entitled "Wild-type Phosphoribosylpyrophosphate Synthase (PRS) from Mycobacterium tuberculosis: a Bacterial Class II PRS?" has been received by PLoS ONE. You will be able to check on the progress of your paper by logging on to Editorial Manager as an author. The URL is http://pone.edmgr.com/.

Your manuscript will be given a reference number once an Editor has been assigned.

Thank you for submitting your work to this journal.

Kind regards,

PLoS ONE

IMPORTANT NOTICE FOR AUTHORS: We would like to forewarn you that there could be a delay in the review time of your manuscript. Our editorial board and reviewers are comprised of faculty and staff from universities around the world, and many of these individuals are away from the office for conferences, holidays or are conducting fieldwork during this time of year. We will do our utmost to process your manuscript in a prompt manner, but please be aware that historically, we have experienced some delays during the summer months. We thank you for your patience in advance, and encourage you to see the following blog post for more information: http://blogs.plos.org/everyone/2011/07/14/summer-service-update/.